NAT'L INST. OF STAND & TECH R.I.C.
A11103 898216

REFERENCE

NIST
PUBLICATIONS

NISTIR 4929

Electronics and Electrical Engineering Laboratory

Technical Publications Announcements

J. A. Gonzalez
Compiler

September 1992

Covering Laboratory Programs,
October to December 1991,
with 1992/1993 EEEL Events Calendar

31

U.S. DEPARTMENT OF COMMERCE
Technology Administration
National Institute of Standards and Technology
Electronics and Electrical Engineering Laboratory
Semiconductor Electronics Division
Gaithersburg, MD 20899

QC
100
.U56
4929
1992

NIST

NIST-IR 93 .U56 4929 1992

NISTIR 4929

Electronics and Electrical Engineering Laboratory

Technical Publications Announcements

Covering Laboratory Programs, October to December 1991, with 1992/1993 EEEL Events Calendar

J. A. Gonzalez
Compiler

September 1992

31

U.S. DEPARTMENT OF COMMERCE
Technology Administration
National Institute of Standards and Technology
Electronics and Electrical Engineering Laboratory
Semiconductor Electronics Division
Gaithersburg, MD 20899

U.S. DEPARTMENT OF COMMERCE
Barbara Hackman Franklin, Secretary

TECHNOLOGY ADMINISTRATION
Robert M. White, Under Secretary for Technology

NATIONAL INSTITUTE OF STANDARDS AND TECHNOLOGY
John W. Lyons, Director

INTRODUCTION TO THE EEEL TECHNICAL PUBLICATION ANNOUNCEMENTS

This is the thirty-first issue of a quarterly publication providing information on the technical work of the National Institute of Standards and Technology Electronics and Electrical Engineering Laboratory (EEEL) (until February 1991, the Center for Electronics and Electrical Engineering). This issue of the EEEL Technical Publication Announcements covers the fourth quarter of calendar year 1991.

Organization of Bulletin: This issue contains citations and abstracts for Laboratory publications published in the quarter. Entries are arranged by technical topic as identified in the Table of Contents and alphabetically by first author within each topic. Following each abstract is the name and telephone number of the individual to contact for more information on the topic (usually the first author). This issue also includes a calendar of Laboratory conferences and workshops planned for calendar year 1992/1993 and a list of sponsors of the work.

Electronics and Electrical Engineering Laboratory: EEEL programs provide national reference standards, measurement methods, supporting theory and data, and traceability to national standards. The metrological products of these programs aid economic growth by promoting equity and efficiency in the marketplace, by removing metrological barriers to improved productivity and innovation, by increasing U.S. competitiveness in international markets through facilitation of compliance with international agreements, and by providing technical bases for the development of voluntary standards for domestic and international trade. These metrological products also aid in the development of rational regulatory policy and promote efficient functioning of technical programs of the Government.

The work of the Laboratory is conducted by four technical research Divisions: the Semiconductor Electronics and the Electricity Divisions in Gaithersburg, Md., and the Electromagnetic Fields and Electromagnetic Technology Divisions in Boulder, Colo. In 1991, the Office of Law Enforcement Standards, formerly the Law Enforcement Standards Laboratory, was transferred to EEEL. This Office conducts research and provides technical services to the U.S. Department of Justice, State and local governments, and other agencies in support of law enforcement activities. In addition, the Office of Microelectronics Programs (OMP) was established in EEEL to coordinate the growing number of semiconductor-related research activities at NIST. Reports of work funded through the OMP are included under the heading "Semiconductor Microelectronics."

Key contacts in the Laboratory are given on the back cover; readers are encouraged to contact any of these individuals for further information. To request a subscription or for more information on the Bulletin, write to EEEL Technical Progress Bulletin, National Institute of Standards and Technology, Metrology Building, Room B-358, Gaithersburg, MD 20899 or call (301) 975-2220.

Laboratory Sponsors: The Laboratory Programs are sponsored by the National Institute of Standards and Technology and a number of other organizations, in both the Federal and private sectors; these are identified on page 28.

Note on Publication Lists: Publication lists covering the work of each division are guides to earlier as well as recent work. These lists are revised and reissued on an approximately annual basis and are available from the originating division. The current set is identified in the Additional Information section, page 26.

TABLE OF CONTENTS

INTRODUCTION .... inside title page

FUNDAMENTAL ELECTRICAL MEASUREMENTS 2

SEMICONDUCTOR MICROELECTRONICS 2
Silicon Materials 2
Compound Materials 4
Device Physics and Modeling 6
Insulators and Interfaces 7
[For Separation by Implanted Oxygen (SIMOX) and for Silicon-on-Insulator (SOI) see Silicon Materials]
Dimensional Metrology 8
Integrated-Circuit Test Structures 9
Microfabrication Technology 9
Power Devices 10
Photodetectors 11
Radiation Effects 11
Other Semiconductor Metrology Topics 11

SIGNAL ACQUISITION, PROCESSING, AND TRANSMISSION 11
DC and Low-Frequency Metrology 11
Waveform Metrology 12
Cryoelectronic Metrology 12
Antenna Metrology 12
[Also see Electromagnetic Interference - Radiated]
Microwave and Millimeter-Wave Metrology 13
Electromagnetic Properties 13
Laser Metrology 14
Optical Fiber Metrology 14
Optical Fiber Sensors 15
Electro-Optic Metrology 15
Complex System Testing 18
Other Signal Topics 18

ELECTRICAL SYSTEMS 18
Power Systems Metrology 18
Magnetic Materials and Measurements 22
Superconductors 23

ELECTROMAGNETIC INTERFERENCE 24
Conducted 24
Radiated 25

ADDITIONAL INFORMATION 26
1992/1993 EEEL CALENDAR 28
EEEL SPONSORS 28
KEY CONTACTS IN LABORATORY, LABORATORY ORGANIZATION .... back cover

FUNDAMENTAL ELECTRICAL MEASUREMENTS

Steiner, R., and Stahley, S., **MAP Voltage Transfer Between 10-V Josephson Array Systems,** Proceedings of the 1991 National Conference of Standards Laboratories Metrology: A Worldwide Language, Albuquerque, New Mexico, August 18-22, 1991, pp. 205-209.

A Measurement Assurance Program (MAP) for voltage transfer at the 10-V level was performed among six U.S. laboratories currently operating 10-V Josephson array systems. A commercial voltage standard based on four Zener references was used as the transfer device. This experiment provided data on the precision and traceable accuracy of the various array systems relative to the national Si-volt representation at the National Institute of Standards and Technology (NIST), as well as on calibrations involving the new multi-Zener reference standards. Preliminary measurements from five other laboratories show that all agree with NIST to within 0.035 parts per million with a maximum random uncertainty of 0.015 parts per million (1 σ).
[Contact: Richard Steiner, (301) 975-4226]

Van Degrift, C.T., Cage, M.E., and Girvin, S.M., Editors, **The Integral and Fractional Quantum Hall Effects,** Resource Letter QHE-1 (American Association of Physics Teachers, College Park, Maryland 1991), pp. 1-15.

This Resource Letter provides a guide to the literature on the integral and fractional quantum Hall effects. The letter E after an item indicates elementary level or material of general interest to persons becoming informed in the field. The letter I, for intermediate level, indicates material of somewhat more specialized nature; and the letter A indicates rather specialized or advanced material. An asterisk (*) indicates articles that are especially useful or interesting; a double asterisk (**) indicates those articles to be included in an accompanying reprint book.
[Contact: Craig T. Van Degrift, (301) 975-4249]

SEMICONDUCTOR MICROELECTRONICS

Silicon Materials

Campisi, G.J., Roitman, P., and Shontz, G.J., **The Role of Annealing Conditions on the Radiation Response of Backgate MOSFETs,** Extended Abstract, Proceedings of the Third Workshop on Radiation-Induced and/or Process-Related Electrically Active Defects in Semincoductor-Insulator Systems, Research Triangle Park, North Carolina, September 10-13, 1991, pp. 171-172 (1991).

SIMOX (Separation by IMplantation of OXygen) is the principal SOI technology used for operation in a radiation environment. The suitability of SIMOX in the submicrometer regime on fully depleted devices depends on the radiation response of the dielectric—the beam synthesized buried oxide. In this study, SOI p-MOSFETs were fabricated on the SIMOX substrates annealed at various times and temperatures. The radiation-induced threshold shifts, ΔV_{bg}, of the gate was determined as a function of substrate processing. Preliminary capacitor studies showed a reduction in the radiation-induced flat-band voltage by 40% when the anneal temperature was increased from 1275 to 1350 °C. The role of anneal temperature on the device properties and radiation response of the buried oxide was investigated in this study. We have correlated the microstructure at the SIMOX interface to the radiation response of the MOSFETs.
[Contact: Peter Roitman, (301) 975-2077]

Campisi, G.J., Roitman, P., Simons, D., and Krull, W.A., **A SIMS Study of the Deuterium Distribution in SIMOX Buried Oxides,** Extended Abstract, Proceedings of the 1991 IEEE International SOI Conference, Vail Valley, Colorado, October 1-3, 1991, pp. 16-17 (1991).

Hydrogen in SiO_2 has been extensively studied and identified as a source of MOS device degradation during hot electron stressing or exposure to ionizing radiation. In this paper, we have used SIMS analysis of deuterium-annealed SIMOX samples to investigate the interaction of hydrogen with the buried oxide.
[Contact: Peter Roitman, (301) 975-2077]

Chi, P.H., Simons, D.S., Roitman, P., and Hughes, H., **Quantitative Depth Profiling of Aluminum-Implanted SIMOX by Use of Secondary Ion Mass Spectrometry,** Microbeam Analysis-1991, D.G. Howitt, ed., pp. 347-349 (1991).

Separation-by-implanted-oxygen (SIMOX) material

has increasingly played an important role in silicon-on-insulator technology because of its radiation-hardening performance and the high-speed and low-power usage of devices made on it. However, the performance of this material can be hampered by the presence, even at low levels, of certain impurities. In this paper, we present the results of secondary ion mass spectrometry by use of the matrix ion species ratio method to quantify Al levels in Al-implanted SIMOX samples.
[Contact: Peter Roitman, (301) 975-2077]

Conley, J.F., Lenahan, P.M., and Roitman, P., **Electron Spin Resonance Study of E′ Trapping Centers in SIMOX Buried Oxides,** IEEE Transactions on Nuclear Science, Vol. 38, No. 6, pp. 1247-1252 (December 1991).

We combine electron spin resonance and capacitance versus voltage measurements with vacuum ultraviolet and ultraviolet illumination sequences to study E′ centers in a variety of SIMOX buried oxides. The oxides had all been annealed above 1300 °C. Our results clearly show that E′ centers play an important, probably dominating, role in the trapping behavior of these oxides. This role is considerably different from the role that E′ centers play in thermal oxides.
[Contact: Peter Roitman, (301) 975-2077]

Conley, J.F., Lenahan, P.M., and Roitman, P., **ESR Study of E′ Trapping Centers in SIMOX Oxides,** Extended Abstract, Proceedings of the 1991 IEEE International SOI Conference, Vail Valley, Colorado, October 1-3, 1991, pp. 12-13 (1991).

We explore E′ trapping centers in separation by implanted oxygen (SIMOX) buried oxides with electron spin resonance (ESR) and capacitance vs. voltage (CV) measurements. Through the use of vacuum-ultraviolet and ultraviolet illumination combined with ESR and CV measurements, we present evidence that E′ centers are important in SIMOX trapping, and that thermal oxide trapping and SIMOX trapping involve different mechanisms.
[Contact: Peter Roitman, (301) 975-2077]

Cortesi, E., El-Ghor, M.K., Hosack, H.H., Allen, L.P., Roitman, P., and Krause, S.J., **Evaluation of Secco Etch Technique for Determination of Dislocation Densities in SIMOX Wafers,** Extended Abstract, Proceedings of the 1991 IEEE International SOI Conference, Vail Valley, Colorado, October 1-3, 1991, pp. 118-119 (1991).

The greatly improved quality of Separation by IMplantation of OXygen (SIMOX) material now being routinely produced has made the measurement of dislocation densities by plan-view transmission electron microscopy extremely impractical because of the large areas that must be studied. We report here on an extensive study of a Secco etch process for determining dislocation densities that was performed by three different groups using nine SIMOX wafers from the same lot.
[Contact: Peter Roitman, (301) 975-2077]

Krause, S.J., Lee, J.D., Chen, B.L., Seraphin, S., Cordts, B., and Roitman, P., **Oxygen Bubble Formation and Evolution During Oxygen Implantation and Annealing of Silicon-on-Insulator Material,** Extended Abstract, Proceedings of the 49th Annual Meeting of the Electron Microscopy Society of America, San Diego, California, August 1991, unpaged (1991).

Silicon-on-insulator material fabricated by high-dose oxygen implantation is a material increasingly used for higher speed and radiation-hard circuits. During implantation, a variety of structural changes occur, including the formation of defects, bubbles, precipitates, and the buried oxide layer. The topic of bubble formation and evolution has received only limited study. Sjoreen et al. first reported the presence of spherical, randomly distributed precipitates near the top surface of the silicon layer. El-Ghor et al. further examined these precipitates and proposed that they were cavities filled with oxygen. Maszara confirmed the presence of spheroids filled with oxygen in the silicon top surface region in the 1 mA cm^{-2} as-implanted samples. In this work, transmission electron microscopy techniques were used to investigate the effect of implantation conditions on the bubble formation and the effect of subsequent annealing conditions on the evolution of bubbles.
[Contact: Peter Roitman, (301) 975-2077]

Park, J.C., Krause, S.J., and Roitman, P., **Microstructural Changes in Oxygen Implanted SOI Material at Intermediate Annealing Steps in Thermal Ramping,** Extended Abstract, Proceedings of the 1991 IEEE International SOI Conference, Vail Valley, Colorado, October 1-3, 1991, pp. 116-117 (1991).

The final microstructure of silicon-on-insulator material fabricated by oxygen implantation (SIMOX) is dependent on the sum of all of the processing steps used to produce the wafer. There have been many reports on microstructures after implantation or annealing, but there is only limited information on microstructural changes occurring during the intermediate stages of processing, in particular, during the thermal ramping cycle. In this work, we are reporting on the microstructural changes in HT SIMOX at various stages in the ramping process by simulating the thermal treatment with 2-h anneals at intermediate temperatures.
[Contact: Peter Roitman, (301) 975-2077]

Thurber, W.R., Lowney, J.R., Larrabee, R.D., and Ehrstein, J.R., **AC Impedance Method for High-Resistivity Measurements of Silicon**, Journal of the Electrochemical Society, Vol. 138, No. 10, pp. 3081-3085 (October 1991).

An ac impedance method for measuring the average bulk resistivity of ingots and slices of high-resistivity silicon is presented. Easily removable contacts, such as silver paint, are applied to the end faces of the sample, and the complex impedance of the resulting capacitive sandwich is measured as a function of frequency. The resistivity can be calculated from the frequency of the negative peak in the imaginary part of the impedance and from the absolute values of the real and imaginary parts at that frequency. The spectroscopic nature of the method gives an inherent separation of contact, surface region, and bulk effects as the respective responses usually occur at widely different frequencies. In addition to its intended application for measuring bulk resistivity, the method is useful for determining the quality of applied contacts and the effect of surface treatments which result in a significant depletion layer. Plots and the required data can be obtained very quickly with an appropriate microprocessor-based impedance analyzer. Extensive measurements of high-resistivity silicon were done to compare the method with the dc resistance, van der Pauw, and four-probe techniques. The agreement was within 5% for slices and ingot sections greater than 0.1 cm in length and resistivity above 5 $k\Omega \cdot cm$.
[Contact: W. Robert Thurber, (301) 975-2067]

Compound Materials

Bennett, H.S., Lowney, J.R., Tomizawa, M., and Ishibashi, T., **Experimentally Verified Majority and Minority Mobilities in Heavily Doped GaAs for Device Simulations**, Extended Abstract, 1991 International Workshop on VLSI Process and Device Modeling (1991 VPAD), Oiso, Japan, May 26-27, 1991, pp. 114-115. [Complete paper will appear in a Special Issue on Selected Papers from '91 VPAD.]

Low-field mobilities and velocity-versus-electric-field relations are among the key input parameters for drift-diffusion simulations of field-effect and bipolar transistors. For example, most device simulations that treat scattering from ionized impurities contain mobilities or velocity-versus-field relations based on the Born approximation (BA). The BA is insensitive to the sign of the charged impurity and is especially poor for ionized impurity scattering because of the relatively strong scattering of long-wavelength carriers, which have low energies, and therefore violate the validity condition for the BA. Such carriers occur at high symmetry points in the Brillouin zone and are critical for device behavior.
[Contact: Herbert S. Bennett, (301) 975-2047]

Dagata, J.A., Tseng, W., Bennett, J., Schneir, J., and Harary, H.H., **P_2S_5 Passivation of GaAs Surfaces for Scanning Tunneling Microscopy in Air**, Applied Physics Letters, Vol. 59, No. 25, pp. 3288-3290 (16 December 1991).

We report a novel method of GaAs substrate preparation which imparts significantly improved topographical and chemical uniformity to the surface. The procedure, employing an aqueous $P_2S_5/(NH_4)_2S$ solution, leaves the surface in a highly ordered state and resistant to air oxidation for periods of a day or more without the presence of foreign chemical layer such as sulfur. Surface quality was determined by scanning tunneling microscopy (STM), time-of-flight secondary ion mass spectrometry, reflection high-energy electron diffraction, and X-ray photoelectron spectroscopy. The remarkable stability and smoothness of treated III-V surfaces is illustrated by STM imaging of an $Al_{0.51}Ga_{0.49}As/GaAs$ superlattice in air. The superlattice consisted of periodic alternating AlGaAs/GaAs layers of various thicknesses from 10 to 1000 nm.
[Contact: Wen F. Tseng, (301) 975-5291]

Doss, M.G., Chandler-Horowitz, D., Marchiando, J.F., Krause, S., and Seraphin, S., **Analysis for the**

Characterization of Oxygen Implanted Silicon (SIMOX) by Spectroscopic Ellipsometry, Proceedings of the Materials Research Society Symposium, Boston, Massachusetts, November 26-December 1, 1990, Vol. 209, pp. 493-498 (1991).

Samples of SIMOX have been prepared using a high-current implanter (density ≈ 1 mA/cm^2) and annealed at 1300 °C for 6 h. Conventional and high-resolution transmission electron microscopy reveal unusual structure in these samples. Spectroscopic ellipsometry has been used to analyze these structures. Ellipsometric measurements were collected at an angle of incidence of 75.5 deg, with energies from 1.5 to 5.0 eV, and using a rotating polarizer configuration. The measurements were analyzed with three models: a three-layer model, a four-layer model, and a five-layer model. The five-layer model provided the best fit of the three. This model identified a layer of crystalline Si inclusions ("islands") within the SiO_2 layer. A method is presented that provides initial estimates for the thickness of the top three layers to help start the regression analysis.
[Contact: Deane Chandler-Horowitz, (301) 975-2084]

Huang, D., Kallergi, M., Aubel, J., Sundaram, S., DeSalvo, G.C., and Comas, J., **Lattice Damage and Atomic Mixing Induced by As^{++} Implantation and Thermal Annealing in AlAs/GaAs Multiple Quantum-Well Structures**, Journal of Applied Physics, Vol. 70, No. 8, pp. 4181-4189 (15 October 1991).

The lattice damage and the nature of the atomic intermixing of Al and Ga induced by As^{++} implantation and thermal annealing in AlAs/GaAs multiple quantum-well structures were investigated. The photoluminescence spectra, which show multiple peaks after implantation and annealing, were analyzed based on the shifts of the excitonic peaks arising from quantum wells located at different depths. The depth profiles of intermixing were obtained using a procedure of successive layer-by-layer chemical etching following photoluminescence measurements. It is found that the mixing is maximum near the sample surface and decreases monotonically with depth, suggesting that the profiles follow the ion-induced damage more closely than the ion density. It is also observed that the damage extends beyond 1 μm. Within 0.3 μm from the surface, the damage is heavy and the atomic intermixing increases rapidly with ion dose, indicating the damage is structural. Beyond 0.3 μm, the degree of intermixing is only sensitive to the anneal temperature but not to the implantation dose. The results show that both direct collisions and interdiffusion are responsible for the atomic mixing. For the samples implanted with ion doses below 10^{14} 1/cm^{-2} and annealed at 650 °C, the optical activation from radiation damage is appreciable. However, the interdiffusion becomes important at temperatures near and above 800 °C.
[Contact: James Comas, (301) 975-2061]

Littler, C.L., Loloee, M.R., Zawadzki, W., and Seiler, D.G., **Bound Hole Excitations in p-$Hg_{0.76}Cd_{0.24}Te$**, Proceedings of the 20th International Conference on the Physics of Semiconductors, Thessaloniki, Greece, August 6-10, 1990, Vol. 3, pp. 2263-226 (1990).

Bound-hole transitions originating from a deep level to light-hole Landau levels have been observed for the first time in HgCdTe. Resonances have been seen in the photovoltaic response of a p-type $Hg_{0.76}Cd_{0.24}Te$ sample subjected to CO_2 laser radiation. The transitions are well described by the Pidgeon-Brown energy band model, yielding an activation energy of 32 ± 2 meV above the valence band edge for the deep level.
[Contact: David G. Seiler, (301) 975-2081]

Littler, C.L., Yoon, I.T., Song, X.N., Zawadzki, W., Pfeffer, P., and Seiler, D.G., **Orbital and Spin Anisotropy of Conduction Electrons in InSb**, Proceedings of the 20th International Conference on the Physics of Semiconductors, Thessaloniki, Greece, August 6-10, 1990, Vol. 3, pp. 1763-1766 (1990).

The anisotropy of the orbital and spin properties of conduction electrons in InSb has been measured simultaneously for the first time using a cyclotron-resonance-type experiment. A novel approach was used to measure precisely small shifts of the resonant field positions with respect to the crystal axes -- the cyclotron resonance signals were detected at the same time from two differently oriented samples. The data have been described using a five-level $k \cdot p$ energy band model, which accounts for both the nonparabolicity and anisotropy of the conduction band in III-V compounds in the presence of a magnetic field.
[Contact: David G. Seiler, (301) 975-2081]

Pellegrino, J., Griffin, J., Myers, L., and Spencer, M., **Beryllium Doping in MBE-Grown GaAs and**

AlGaAs, Proceedings of the Materials Research Society Symposium, Boston, Massachusetts, November 27-December 2, 1989, Vol. 163, pp. 881-886 (1990).

Beryllium is an effective p-dopant in GaAs and AlGaAs and plays an important role in device characterizations of heterobipolar transistors. This work addresses the doping and mobility properties for two series of beryllium-doped samples: GaAs and AlGaAs. Within each series the doping ranged between levels of $3 \times 10^{15}cm^{-3}$ to $5 \times 10^{19}cm^{-3}$. Mobility and carrier concentrations were obtained through Hall and Polaron measurements. The doping concentration results suggest the onset of carrier compensation at higher doping levels. One possible explanation is that for high doping levels, Be is incorporated as interstitial donors. A thermodynamic model is used to explain the observations.
[Contact: Joseph G. Pellegrino, (301) 975-2123]

Device Physics and Modeling

Bennett, H.S., Lowney, J.R., Tomizawa, M., and Ishibashi, T., **Experimentally Verified Majority and Minority Mobilities in Heavily Doped GaAs for Device Simulations**, Extended Abstract, 1991 International Workshop on VLSI Process and Device Modeling (1991 VPAD), Oiso, Japan, May 26-27, 1991, pp. 114-115. [Complete paper will appear in a Special Issue on Selected Papers from '91 VPAD.]

Low-field mobilities and velocity-versus-electric-field relations are among the key input parameters for drift-diffusion simulations of field-effect and bipolar transistors. For example, most device simulations that treat scattering from ionized impurities contain mobilities or velocity-versus-field relations based on the Born approximation (BA). The BA is insensitive to the sign of the charged impurity and is especially poor for ionized impurity scattering because of the relatively strong scattering of long-wavelength carriers, which have low energies, and therefore violate the validity condition for the BA. Such carriers occur at high symmetry points in the Brillouin zone and are critical for device behavior.
[Contact: Herbert S. Bennett, (301) 975-2047]

Lowney, J.R., and Mayo, S., **Analysis of Persistent Photoconductivity Due to Potential Barriers**, Proceedings of the Third Workshop on Radiation-Induced and/or Process-Related Electrically Active Defects in Semiconductor-Insulator Systems, Research Triangle Park, North Carolina, September 10-13, 1991, pp. 95-102.

Persistent photoconductivity has been seen in thin silicon resistors fabricated with SIMOX material at temperatures between 60 and 220 K. This effect has been attributed to the depletion of carriers near the interface between the top silicon layer and the buried oxide, which is due to the large number of surface traps at this interface. The depletion of carriers is accompanied by a built-in field on the order of 10,000 V/cm, which causes a potential barrier that is about a quarter of the energy gap of silicon. The theory of the recombination kinetics of majority carriers with minority carriers trapped at the interface on the other side of a potential barrier is studied. Both the possibilities of tunneling and thermal activation have been considered. The results show that thermal activation dominates at the temperatures of the NIST measurements in SIMOX material, while at lower temperatures tunneling would dominate.
[Contact: Jeremiah R. Lowney, (301) 975-2048]

Mitter, C.S., Hefner, A.R., Jr., Chen, D.Y., and Lee, F.C., **Insulated Gate Bipolar Transistor (IGBT) Modeling Using IG-Spice**, Proceedings of the 1991 IEEE Industry Applications Society Meeting, Dearborn, Michigan, September 28-October 4, 1991, pp. 1515-1521.

A physics-based model for the Insulated Gate Bipolar Transistor (IGBT) is implemented into the widely available circuit simulation package IG-Spice. Based on analytical equations describing the semiconductor physics, the model accurately describes the nonlinear junction capacitances, moving boundaries, recombination, and carrier scattering, and effectively predicts the device conductivity modulation. In this paper, the procedure used to incorporate the model into IG-Spice and various methods necessary to ensure convergence are described. The effectiveness of the Spice-based IGBT model is demonstrated by investigating the static and dynamic current sharing of paralleled IGBTs with different device model parameters. The simulated results are verified by comparison with experimental results.
[Contact: Allen R. Hefner, Jr., (301) 975-2071]

Tomizawa, M., Ishibashi, T., Bennett, H.S., and

Lowney, J.R., **Verification of Effective Intrinsic Carrier Concentrations for Numerical Simulations of Gallium Arsenide Bipolar Transistors**, Extended Abstract, Proceedings of the 1991 International Workshop on VLSI Process and Device Modeling (1991 VPAD), Oiso, Japan, May 26-27, 1991, pp. 116-117.

Using the best available physical models is essential for predictive numerical simulations of heterostructure GaAs bipolar transistors. Recent theoretical calculations of n_{ie} for GaAs at 300 K have been verified experimentally for the first time by measurements on devices.
[Contact: Herbert S. Bennett, (301) 975-2047]

Insulators and Interfaces
[For Separation by Implanted Oxygen (SIMOX) and for Silicon-on-Insulator (SOI) see Silicon Materials]

Kim, K.H., Bell, M.I., Dozier, C.M., Freitag, R.K., and Bouldin, C.E., **Correcting for X-Ray Energy Calibration Error Caused by Misalignment of a Right-Angle Linkage Monochromator** [original title: Correcting for Error Caused by Misalignment of Right-Angle Linkage Monochromator], Review of Scientific Instrumentation, Vol. 62, No. 4, pp. 982-985 (April 1991).

Small alignment errors of right-angle linkage monochromators typical to many XAFS beamlines can cause significant errors in the energy calibrations. A 1-deg misalignment produces errors greater than 1 keV over the hard X-ray operating range of a typical monochromator. The energy error caused by such misalignments is analyzed and its mathematical form given. The error can be corrected by inverting the expression, and the amount of misalignment determined by accurate energy measurements at a few points. The accuracy of the corrections is tested. The effects of this error on X-ray absorption fine structure data and their interpretation are also discussed.
[Contact: David G. Seiler, (301) 975-2081]

Mayo, S., Lowney, J.R., and Roitman, P., **Measurement of Interface Defects in Gated SIMOX Structures**, Extended Abstract, Proceedings of the 1991 IEEE International SOI Conference, Vail Valley, Colorado, October 1-3, 1991, pp. 52-53.

Defects in gated or ungated thin film resistors have been characterized by photoinduced transient spectroscopy (PITS). The resistors were fabricated with n- or p-type SIMOX (separation by implanted oxygen) wafers implanted with 200-keV oxygen to 1.8 x 10^{18} cm^{-2} total fluence. One wafer used for gated resistor fabrication was implanted at 595 °C and sequentially annealed at 1325 °C for 4 h in argon (plus 0.5% oxygen) followed by 4 h in nitrogen (plus 0.5% oxygen). Another wafer used for ungated resistor fabrication was implanted at 650 °C and annealed at 1275 °C for 2 h in nitrogen (plus 0.5% oxygen). PITS data indicate that electron or hole traps in the conductive silicon film are located at the film-buried silica interface. We estimate the average interface trap density in the SIMOX structure to be in the 10^{11} cm^{-2} range.
[Contact: Santos Mayo, (301) 975-2045]

Richter, M., Woicik, J.C., Pianetta, P., Miyano, K.E., Kendelewicz, T., Bouldin, C.E., Spicer, W.E., and Lindau, I., **Surface Extended X-Ray Adsorption Fine Structures Studies of the Si(001) 2×1-Sb Interface**, Journal of Vacuum Science Technology A, Vol. 9, No. 3, pp. 1951-1955 (May/Jun 1991).

Surface X-ray adsorption fine structure (SEXAFS) has been used to investigate the structure of Sb on the Si(001) 2 x 1 surface. The coverage of Sb which remains after annealing thick layers at 375 °C, previously reported to be one monolayer (ML), is found in this work to form a disordered overlayer with three-dimensional Sb clusters. This finding is concluded from the Sb L_3 absorption spectra which are similar for this coverage to that of bulk Sb. After a 550 °C anneal, Auger electron spectroscopy and scanning tunneling microscopy (STM) show that about one ML of Sb remains. Phase and amplitude analysis of the Sb L_3 edge SEXAFS shows that the remaining Sb atoms occupy a modified bridge site with a Si-Sb bond length of 2.63 ± 0.04 Å. The Sb atoms form dimers with a Sb-Sb bond length of 2.91 ± 0.04 Å, which is almost identical to the bulk Sb-Sb bond length of 2.90 Å. The Sb atoms lie 1.74 ± 0.06 Å above the Si(001) surface. STM confirms the dimer structure of the Sb overlayer. Low-energy electron diffraction performed on vicinal single-domain Si show that these dimers form rows that run perpendicular to the Si dimer rows.
[Contact: David G. Seiler, (301) 975-2431]

Woicik, J.C., Bouldin, C.E., Bell, M.I., Cross,

J.O., Tweet, D.J., Swanson, B.D., Zhang, T.M., Sorensen, L.B., King, C.A., Hoyt, J.L., Pianetta, P., and Gibbons, J.F., **Conservation of Bond Lengths in Strained Ge-Si Layers**, Physical Review B, Vol. 43, No. 3, pp. 2419-2422 (15 February 1991).

The combined techniques of X-ray absorption fine structure (EXAFS) and X-ray diffraction have been used to study the strain and bond distortions in epitaxial GeSi on Si(001). In a 31%-Ge, 340-Å pseudomorphic GeSi film, the Ge-Ge and Ge-Si first-neighbor bond lengths have been found to be 2.44 ± 0.02 Å and 2.38 ± 0.02 Å, respectively. The lattice parameter perpendicular to the GeSi/Si(001) interface has been found to be $a_\perp = 5.552 \pm 0.002$ Å, in agreement with the predictions of macroscopic elastic theory. These results show that the bond length strain in the epitaxial layer appears in the second and higher coordination shells, rather than in the nearest neighbor bond lengths which remain the same as in unstrained GeSi. A microscopic model is presented which accounts for these findings.
[Contact: David G. Seiler, (301) 975-2046]

Woicik, J.C., Kendelewicz, T., Miyano, K.E., Bouldin, C.E., Meissner, P.L., Pianetta, P., and Spicer, W.E., **Local Bonding Structure of Sb on Si(111) by Surface Extended X-Ray Absorption Fine Structure and Photoemission**, Physical Review B, Vol. 43, No. 5, pp. 4331-4339 (15 February 1991).

The combined techniques of surface extended X-ray absorption fine structure (SEXAFS) and high-resolution core and valence photoelectron spectroscopy have been used to study the local bonding structure of the Sb/Si(111) interface. From photoemission, we find that the Sb atoms absorb in a unique environment which completely saturates the dangling bonds of the Si(111) surface, and which completely eliminates the surface components of the Si 2p core level spectrum. The Sb-induced Si 2p interfacial core level shift has been found to be shifted 0.20 ± 0.02 eV towards higher binding energy with an intensity which corresponds to 1 ml of surface atoms. The SEXAFS determination of the absolute surface coordination numbers and bond lengths within the first Sb shell is 2.1 ± 0.3 Sb atoms at 2.86 ± 0.02 Å and 2.0 ± 0.4 Si atoms at 2.66 ± 0.03 Å. Combined, these results indicate that Sb trimmers occupy the threefold atop sites of the Si(111) surface where each Sb atom is bonded to two Si atoms in a modified bridge configuration.
[Contact: David G. Seiler, (301) 975-2081]

Woicik, J.C., Kendelewicz, T., Miyano, K.E., Bouldin, C.E., Meissner, P.L., Pianetta, P., and Spicer, W.E., **Structure of the Si(111) $\sqrt{3}$x$\sqrt{3}$-Sb Interface by Surface X-Ray Absorption Fine Structure and Photoemission,** Journal of Vacuum Science Technology A, Vol. 9, No. 3, pp. 1956-1961 (May/Jun 1991). [Proceedings of the American Vacuum Society Meeting, Toronto, Canada, October 8-12, 1990.]

The combined techniques of surface extended X-ray absorption fine structure (SEXAFS) and high-resolution core level photoelectron spectroscopy have been used to investigate the local bonding structure of the Sb/Si(111) interface. We find that the adsorption of 1 monolayer (ML) of Sb completely eliminates the surface components of the Si 2p core level spectrum. The Sb-induced Si 2p interfacial core level has been found to be shifted 0.20 ± 0.02 eV towards higher binding energy with an intensity that corresponds to the top 1 ML of surface atoms. The SEXAFS determination of the absolute surface coordination numbers and bond lengths within the first Sb shell is 2.1 ± 0.3 Sb atoms at 2.86 ± 0.02 Å and 2.0 ± 0.4 Si atoms at 2.66 ± 0.03 Å. Together, these results indicate that Sb trimers occupy the threefold atop sites of the Si(111) surface where each Sb atom is bonded to two Si atoms in a modified bridge configuration.
[Contact: David G. Seiler, (301) 975-2081]

Dimensional Metrology

Larrabee, R.D., Linholm, L.W., and Postek, M.T., **Submicrometer Critical Dimension Metrology,** "Handbook of VLSI Microlithography," Chapter 3, pp. 148-237 (Noyes Publications, Park Ridge, New Jersey, 1991).

The never-ending push of the semiconductor industry toward submicrometer feature sizes on integrated circuits and in discrete devices has led to the situation where the development of the techniques of fabrication of submicrometer features has exceeded the development of the metrological techniques required to accurately measure and characterize these features. At the present time (1987), there are no submicrometer critical-dimension standards available from the National Institute of Standards and Technology

(NIST) for feature-size measurements on integrated circuits and thus, no way to achieve traceability to NIST for such measurements. NIST has active programs to develop the techniques for measuring such features and for certifying standards using optical microscopy and scanning electron microscopy. In addition, NIST has an active program to develop electrical dimensional metrology using specially designed test patterns. This chapter summarizes these programs and highlights some of the results obtained to date. This chapter does not discuss some of the potential or proposed techniques of dimensional metrology that might be used in the more distant future (e.g., scanning tunneling microscopy) and does not evaluate any of the proposed nonconventional modes of operation of the optical or scanning-electron microscopes (e.g., near-field optical imaging). The purpose of the chapter is to describe the general state of the art in submicrometer dimensional metrology as presently practiced by the semiconductor industry, to highlight some of the problems with such practice, and to give suggestions on how to improve the precision and accuracy of such measurements.
[Contact: Robert D. Larrabee, (301) 975-2298]

Postek, M.T., and Keery, W.J., **Cryopump Vibration Isolation System for an SEM**, Scanning, Vol. 13, pp. 404-409 (1991).

A standard commercially available cryopump system has been installed on a scanning electron microscope (SEM) using specially optimized vacuum vibration isolation bellows. This installation was successful in reducing the cryopump-induced vibration to a level that did not degrade the standard performance or resolution of the SEM in the pump-on mode and, in the pump-off (or coasting) mode, eliminated all measurable instrument-induced vibration (i.e., from the vacuum system). This paper outlines the manner in which this performance has been accomplished, and presents the results of an experiment demonstrating the reduction of specimen contamination provided by this type of vacuum system.
[Contact: Michael T. Postek, (301) 975-2299]

Integrated-Circuit Test Structures

Schuster, C.E., Linholm, L.W., and Gillespie, J.K., **High-Density Test Structures for Assessing Microwave/Millimeter Wave Monolithic Integrated Circuit (MIMIC) Performance**, Digest of Papers, Proceedings of the 1991 Government Applications Conference (GOMAC), Orlando, Florida, November 5-7, 1991, Vol. XVII, pp. 335-338.

This paper discusses the unique, high-density implementation of microelectronic test structures used to diagnose and predict MIMIC performance under MIMIC Phase 1, Task 4.E. It also presents assessments and recommendations, based on Task 4.E data, to improve and extend current parametric test structure methods for use in future efforts to correlate and monitor MIMIC material, process, and device characteristics.
[Contact: Constance E. Schuster, (301) 975-2241]

Troccolo, P., Mantalas, L., Allen, R.A., and Linholm, L.W., **Extending Electrical Measurements to the 0.5 μm Regime**, Proceedings of SPIE (The International Society for Optical Engineering, P.O. Box 10, Bellingham, Washington 98227-0010), Integrated Circuit Metrology, Inspection, and Process Control V, Vol. 1464, pp. 90-103 (1991).

The purpose of this work was to extend the design criteria of electrical test structures to the half-micrometer linewidth region. At 0.5 μm, process limitations place constraints on the functionality and usefulness of electrical test structures based on conventional design criteria. In particular, small total variations from lens aberrations/distortions and proximity/corner rounding effects in the patterning of the smallest lines achievable (less than 0.5 μm) can result in structure failure. This was particularly significant when orthogonal voltage taps at minimum design geometries were used. As geometries decrease in size and control over the process and equipment tightens, the intrinsic error in conventional structures has increased as a percentage of the total measurement. The design criteria of these structures have been further modified and improved in order to address known lithographic limitations and establish a more process-tolerant design. The resulting measurement precision accommodating these changes is discussed to provide the framework for achieving the highest practical performance attainable from both the test structure and the measurement system.
[Contact: Richard A. Allen, (301) 975-5026]

Microfabrication Technology

Dagata, J.A., Tseng, W., Bennett, J., Schneir, J.,

and Harary, H.H., **Nanolithography on III-V Semiconductor Surfaces Using a Scanning Tunneling Microscope Operating in Air**, Journal of Applied Physics, Vol. 70, No. 7, pp. 3661-3665 (1 October 1991).

Nanometer-scale pattern generation on III-V semiconductor substrates using a scanning tunneling microscope (STM) operating in air is demonstrated. The sample substrates, consisting of arsenic-capped, epitaxial layers of n-doped GaAs, $Al_xGa_{1-x}As$ and $In_yGa_{1-y}As$ were prepared by molecular beam epitaxy and characterized by time-of-flight secondary-ion mass spectrometry and X-ray photoelectron spectroscopy. The direct patterning of features of width ≤50 nm on GaAs and $In_{0.2}Ga_{0.8}As$ surfaces is shown to be the result of the formation of a strongly bonded surface oxide induced under high electric-field conditions existing between the scan tip and the substrate. The significance of STM pattern generation of nanometer-scale oxide masks for use in the fabrication of low-dimensional heterostructures is discussed.
[Contact: Wen F. Tseng, (301) 975-5291]

Parameswaran, M., Chung, R., Gaitan, M., Johnson, R.B., and Syrzycki, M., **Commercial CMOS Fabricated Integrated Dynamic Thermal Scene Simulator**, Technical Digest, 1991 International Electron Devices Meeting (IEDM), Washington, D.C., December 8-11, 1991, pp. 29.4.1-19.4.4 (1991).

We report a prototype integrated dynamic thermal scene simulator chip, consisting of a 2 by 2 array of integrated thermal pixels. The chips were fabricated using commercial CMOS processes available through vendor services. The micromachining process, needed to create the thermally isolated structures, is introduced as a maskless post-processing step. The thermal pixel and the control electronics are designed as a module for an easy implementation of the array. Test results indicate that the pixels have a thermal time constant of 5 ms and are capable of producing an infrared output of apparent radiometric temperatures in excess of 600 °C and color temperatures of at least 500 °C. The control electronics is capable of switching within 900 ns, enabling the addressing of multiple pixels within the 200-Hz frame time required for a typical dynamic thermal scene simulation.
[Contact: Michael Gaitan, (301) 975-2070]

Pellegrino, J.G., Qadri, S., Tseng, W.F., and Comas J., **Periodicities Associated with Low-Order AlAs/GaAs Superlattices**, Journal of Thin Solid Films, Vol. 206, pp. 40-46 (1991).

The use of MBE to produce heterostructures has made it possible to examine superlattices with monolayer and submonolayer period spacings. In this work we examine the physical properties for the superlattice system (GaAs)n1(AlAs)n2/GaAs(001) for low values of n1 and n2, i.e., n1 = n2 = 3,6,12. Normal, interrupted growth, and migration-enhanced epitaxy growth techniques were used to grow superlattice structures, and X-ray diffraction was used to analyze the major and satellite peak positions. An analysis of the major diffraction peaks and their associated satellites exhibited superlattice periodicity in good agreement with theory. Diffraction peaks were also observed in regions adjacent to the primary diffraction peaks which did not occur in the expected satellite positions. An analysis of these peaks relative to the primary peaks indicate periodicities which are greater than the intended period. One possible cause for these periodicities is variations in growth conditions which occur while the superlattice is being grown. An understanding of low-order superlattices is important for structures which are dependent upon interface sharpness.
[Contact: Joseph G. Pellegrino, (301) 975-2123]

Power Devices

Blackburn, D.L., **Failure Mechanisms and Nondestructive Testing of Power Bipolar and MOS Gated Transistors**, Proceedings of the EPE - MADEP '91/MADEP Symposium on Materials and Devices for Power Electronics, 4th European Conference on Power Electronics and Applications, Florence, Italy, September 2-6, 1991, pp. 0-252 to 0-257.

Failure mechanisms and nondestructive testing of power bipolar and MOS-gated devices are discussed. Bipolar transistor failures are initiated at relatively low temperatures, and these devices can be tested nondestructively. Modern MOS-gated device failure is initiated at temperatures far in excess of those normally considered safe and cannot be tested nondestructively today. The key to nondestructive testing is the ability to sense the onset of failure and to then remove all power from the transistor before the device temperature rises high enough to cause dam-

age.
[Contact: David L. Blackburn, (301) 975-2068]

Photodetectors

Geist, J., Chandler-Horowitz, D., Kohler, R., Robinson, A.M., and James, C.R., **Numerical Modeling of Short-Wavelength Internal Quantum Efficiency**, Metrologia, Vol. 28, pp. 193-196 (1991).

Results of numerical modeling of short-wavelength, internal quantum efficiency of various types of silicon photodiode are presented. The important conclusions are: 1) Interpreting the data obtained from oxide-bias experiments with the help of numerical quantum efficiency models will provide higher accuracy than can be obtained from the conventional self-calibration formula. 2) For high-quality silicon photodiodes, the spectral shape of the internal quantum deficiency (one minus the quantum efficiency) is virtually independent of the density of charge trapped in the oxide and of the surface-recombination velocity at the oxide-silicon interface.
[Contact: Jon Geist, (301) 975-2066]

Radiation Effects

Campisi, G.J., Roitman, P., and Shontz, G.J., **The Role of Annealing Conditions on the Radiation Response of Backgate MOSFETs**, Extended Abstract, Proceedings of the Third Workshop on Radiation-Induced and/or Process-Related Electrically Active Defects in Semiconductor-Insulator Systems, Research Triangle Park, North Carolina, September 10-13, 1991, pp. 171-172 (1991).

SIMOX (Separation by IMplantation of OXygen) is the principal SOI technology used for operation in a radiation environment. The suitability of SIMOX in the submicrometer regime on fully depleted devices depends on the radiation response of the dielectric—the beam synthesized buried oxide. In this study, SOI p-MOSFETs were fabricated on the SIMOX substrates annealed at various times and temperatures. The radiation-induced threshold shifts, ΔV_{bg}, of the gate was determined as a function of substrate processing. Preliminary capacitor studies showed a reduction in the radiation-induced flat-band voltage by 40% when the anneal temperature was increased from 1275 to 1350 °C. The role of anneal temperature on the device properties and radiation response of the buried oxide was investigated in this study. We have correlated the microstructure at the SIMOX interface to the radiation response of the MOSFETs.
[Contact: Peter Roitman, (301) 975-2077]

Other Semiconductor Metrology Topics

Parameswaran, M., Chung, R., Gaitan, M., Johnson, R.B., and Syrzycki, M., **Commercial CMOS Fabricated Integrated Dynamic Thermal Scene Simulator**, Technical Digest, 1991 International Electron Devices Meeting (IEDM), Washington, D.C., December 8-11, 1991, pp. 29.4.1-19.4.4 (1991).

We report a prototype integrated dynamic thermal scene simulator chip, consisting of a 2 by 2 array of integrated thermal pixels. The chips were fabricated using commercial CMOS processes available through vendor services. The micromachining process, needed to create the thermally isolated structures, is introduced as a maskless post-processing step. The thermal pixel and the control electronics are designed as a module for an easy implementation of the array. Test results indicate that the pixels have a thermal time constant of 5 ms and are capable of producing an infrared output of apparent radiometric temperatures in excess of 600 °C and color temperatures of at least 500 °C. The control electronics is capable of switching within 900 ns, enabling the addressing of multiple pixels within the 200-Hz frame time required for a typical dynamic thermal scene simulation.
[Contact: Michael Gaitan, (301) 975-2070]

SIGNAL ACQUISITION, PROCESSING, AND TRANSMISSION

DC and Low-Frequency Metrology

Elmquist, R.E., and Dziuba, R.F., **Isolated Ramping Current Sources for a Cryogenic Current Comparator Bridge**, Review of Scientific Instrumentation, Vol. 62, No. 10, pp. 2457-2460 (October 1991).

The design and performance of a pair of highly isolated ramping and reversing direct current sources for use with a cryogenic current comparator resistance bridge and dc SQUID detector are described. The current sources are floating and isolated from each other, and are internally programmed to reverse the output current while maintaining the SQUID feed-

back control system in lock. Sources have been constructed with full-scale current ranges from 0.65 mA to 100 mA and have been used in the comparisons of precision standard resistors at the 0.01 parts-per-million level.
[Contact: Randolph E. Elmquist, (301) 975-6591]

Waveform Metrology

Chesnut, S.M., and Paulter, N.G., **Automatic Waveform Analysis and Measurement System User Manual,** NISTIR 3978 (December 1991).

The theory and operation of an upgraded version of the National Institute of Standards and Technology (NIST) Automatic Waveform Analysis and Measurement System (AWAMS) is described. This system was commissioned by the Army Primary Standards Laboratory to facilitate measurement comparability with NIST. The AWAMS has been installed at Redstone Arsenal, Alabama.
[Contact: S. Michelle Chesnut, (303) 497-3456]

Oldham, N.M., Hetrick, P.S., Kramar, J., Penzes, W., Wheatley, T., and Teague, C., **Electronic Limitations in Phase Meters for Heterodyne Interferometry,** Proceedings of the Sixth Annual Conference of the American Society for Precision Engineering, Santa Fe, New Mexico, October 13-18, 1991, pp. 47-49.

Reasonable attention has been given to the fidelity of the process by which heterodyne interferometers convert optical path difference between beams that have traversed a test leg and a reference leg, respectively, to a phase difference between electrical signals from the reference and test photodetectors. This paper reports on a study of the next step: to obtain a quantitative result from these signals by measuring the electrical phase difference between the two photodetector signals.
[Contact: Nile M. Oldham, (301) 975-2408]

Cryoelectronic Metrology

Benz, S.P., and Burroughs, C.J., **Two-Dimensional Arrays of Josephson Junctions as Voltage-Tunable Oscillators,** Superconductor Science Technolgy, Vol. 4, pp. 561-567 (1991).

We have detected coherent emission from two-dimensional arrays of superconductor-insulator-superconductor Josephson junctions. Two-dimensional arrays emit coherent radiation over a frequency range of 60 to 210 GHz, when coupled to detector junctions through dc-blocking capacitors. The detector junctions exhibit Shapiro steps at frequencies corresponding to the voltage across single-array junctions. The maximum power from a 10-by-10 junction array coupled to a detector junction occurs at 150 GHz and is estimated to be 0.4 μW, based on simulations of the detector circuit. By varying the number of array junctions, the array geometry, the junction critical urrent, and the coupling circuit, we have begun determining the essential conditions for observing coherent emission.
[Contact: Sam P. Benz, (303) 497-5258]

Hamilton, C.A., and Gilbert, K.C., **Margins and Yield in Single Flux Quantum Logic,** IEEE Transactions on Applied Superconductivity, Vol. 1, No. 4, pp. 157-163 (December 1991).

Simulations are used to optimize the design of simple rapid-single-flux quantum (RSFQ) logic gates and to determine their margins. Optimizations based on maximizing the smallest (critical) margin result in critical margin values in the range 19 to 50%. A Monte Carlo approach is used to illustrate the relationship between margins and process yield. Based on single gate results, the results show that one sigma parameter spreads of less than about ±5% will be required to make medium- or large-scale integrated RSFQ logic circuits. Finally, a single-bit full adder using five RSFQ gates and a local self-timing network is simulated at the discrete component level. The full adder used 2000 A/cm^2 junctions with a specific capacitance of 0.04 pF/μm^2 and had a logic delay of 87 ps and a worst-case margin of ±10%. These results show that margin calculations on individual gates are not necessarily representative of the performance of these gates in complex networks.
[Contact: Clark A. Hamilton, (303) 497-3740]

Antenna Metrology
[Also see Electromagnetic Interference - Radiated]

Francis, M.H., and Wittmann, R.C., **Swept Frequency Gain Measurements From 33 to 50 GHz at the National Institute of Standards and Technology,** Proceedings of the Antenna Measurement Techniques Association Meeting, Boulder, Colorado,

October 7-11, 1991, pp. 1-3 to 1-16.

As part of an effort to provide improved measurement services at frequencies above 30 GHz, scientists at the National Institute of Standards and Technology have completed development of a swept frequency gain measurement service for the 33- to 50-GHz band. This service gives gain values with an accuracy of ±0.3 dB. In this paper, we discuss an example measurement and the associated errors.
[Contact: Michael H. Francis, (303) 497-5873]

Repjar, A.G., Kremer, D.P., Guerrieri, J.R., and Canales, N., **Determining Faults on a Flat Phased Array Antenna Using Planar Near-Field Techniques,** Proceedings of the Antenna Measurements Technique Association Meeting, Boulder, Colorado, October 7-11, 1991, pp. 8-11 to 8-19.

The Antenna Metrology Group of the National Institute of Standards and Technology (NIST) has recently developed and implemented measurement procedures to diagnose faults on a flat phased-array antenna. First, the antenna was measured on the NIST planar near-field (PNF) range, taking measurements on a plane where the multiple reflections between the probe and the antenna under test are minimized. This is important since the PNF method does not directly allow for their effects. Then, the NIST PNF software which incorporates the fast Fourier transform (FFT) was used to determine the antenna's gain and pattern, and to evaluate the antenna's performance. Next, the inverse FFT was used to calculate the fields at the aperture plane. By using this technique, errors in the aperture fields due to multiple reflections can be avoided. By analyzing these aperture plane data through the use of detailed amplitude and phase contour plots, faults in the antenna were located and corrected. The PNF theory and utilization of the inverse FFT is briefly discussed and results are shown.
[Contact: Andrew G. Repjar, (303) 497-5703]

Microwave and Millimeter-Wave Metrology

Judish, R.M., and Burns, J.G., **Measurement Program Compares Automatic Vector Analyzers** [original title: ARFTG Sponsors Measurement Comparison Program], Microwaves & RF, pp. 203-ff (May 1991).

The Automated Radio Frequency Techniques Group (ARFTG) has developed a program that provides ARFTG members the opportunity to compare the performance of their automatic network analyzers to that of their peers. This program is called the Measurement Comparison Program. Participants are provided an analysis of their measurement results in comparison to measurements made at other laboratories.
[Contact: Robert M. Judish, (303) 497-3380]

Wittmann, R.C., and Yaghjian, A.D., **Spherical-Wave Expansions for Piston-Radiator Fields,** Journal of the Acoustical Society of America, Vol. 90, No. 3, pp. 1647-1655 (September 1991).

Simple spherical-wave expansions for the continuous-wave fields of a circular piston radiator in a rigid baffle are derived. These expansions are valid throughout the illuminated half space and are useful for efficient numerical computation in the near-field region. Multipole coefficients are given by closed-form expressions which can be evaluated recursively.
[Contact: Ronald C. Wittmann, (303) 497-3326]

Electromagnetic Properties

Ondrejka, A.R., and Kanda, M., **A Time-Domain Method for Measuring the Reflection Coefficient of Microwave Absorbers at Frequencies Below 1 GHz,** 1991 Digest, Antennas and Propagation Society Symposium, London, Ontario, Canada, June 24-28, 1991, Vol. 3, pp. 1656-1663.

A wideband time-domain reflectometer is used to evaluate the reflection characteristics of rf/microwave absorbers. The reflectometer uses an array of two identical broadband antennas, both transmitting and receiving. The method uses the two antennas in a difference mode to remove the undesired signals and enhance the small reflections being measured. Using this technique, we can separate front-surface reflections from those which are generated at greater angles. The bandwidth of our pulses is 30 MHz to 1000 MHz, and reflection characteristics are measured over this range. The method has been used to characterize the reflectivity of three different types of absorber placed in an anechoic chamber. The results are reported together with the measurement accuracy.
[Contact: Arthur R. Ondrejka, (303) 497-3309]

Laser Metrology

Sanford, N.A., Malone, K.J., and Larson, D.R., **Extended-Cavity Operation of Rare-Earth Doped Glass Waveguide Lasers** [original title: Extended-Cavity Operation of Glass Integrated-Optic Lasers: Mode-Locking, Q-Switching, and Wavelength Tuning], Optics Letters, Vol. 16, No. 14, pp. 1095-1097 (July 15, 1991). [Proceedings of the Integrated Photonics Research Conference, Monterey, California, April 9-11, 1991.]

Integrated-optic lasers have been operated, pulsed and cw, using extended cavities. The results are: mode-locked pulse widths of roughly 80 ps, 1.2 W of Q-switched peak power, and tuning from 1050 to 1074 nm with approximately 7-GHz linewidth.
[Contact: Norman A. Sanford, (303) 497-5239]

Optical Fiber Metrology

Danielson B.L., **Precise Length Measurements in Multimode Optical Fibers** [original title: Precision Length Measurements in Multimode Optical Fibers], Applied Optics, Vol. 30, No. 27, pp. 3867-3872 (20 September 1991).

By using selective optical excitation, both the group index and group delay of on-axis modes of multimode fibers can be determined with high precision. The group index of several types of fibers was measured at 1310 nm in a fiber Michelson interferometer, and the values tabulated. Group delays were obtained from the transit time of short duration optical pulses. From these data, the length of reference fibers about 2 km long was calculated. Length measurement accuracy was limited by group index uncertainties to about 0.04%. Also, a technique is described which uses these reference fibers to minimize uncertainties in distance measurements made with multimode optical time domain reflectometers.
[Contact: Bruce L. Danielson, (303) 497-5620]

Gallawa, R.L., Goyal, I.C., and Ghatak, A.K., **Optical Waveguide Analysis Using Modified Airy Functions**, Fiber and Integrated Optics, Vol. 10, pp. 1-10 (1991).

We review a little-used but powerful method of solving one of the most fundamental equations of mathematical physics. The method is not new, but it is apparently not familiar to the optics community. It uses a modification of the well-known Airy functions, which are easily calculated on desktop computers. We review the method through examples which have an exact solution. We trust that this review will serve to stimulate further examination of a method that seems to have considerable promise.

The method that we review here is reminiscent of the WKBJ methodology (commonly known as the WKB approximation. WKBJ refers to the initials of four independent workers, Wentzel, Kramers, Brillouin, and Jeffrey, who first used the approximation procedure to solve the Schroedinger wave equation in one dimension), but the solution, although approximate, is much more useful than the traditional WKBJ solution and can be used with almost as much ease. The method is extremely powerful but, to our knowledge, is not being used by the optics community, where its use in analyzing optical fibers and integrated optical waveguides would be beneficial.
[Contact: Robert L. Gallawa, (303) 497-3761]

Mechels, S., and Young, M., **Scanning Confocal Microscope for Precise Measurement of Optical Fiber Diameter**, Proceedings of SPIE (The International Society for Optical Engineering, P.O. Box 10, Bellingham, Washington 98227-0010), Scanning Microscopy Instrumentation, Vol. 1556, pp. 164-170 (1992).

We have constructed and evaluated a scanning confocal microscope for the precise measurement of optical fiber cladding diameter. The system measures the fiber endface directly and differs from conventional microscopes in that it minimizes the systematic error due to partial coherence. The results obtained with the scanning confocal microscope are checked by comparison with those obtained from a contact micrometer and by measuring a chrome-on-glass Standard Reference Material provided by NIST, Gaithersburg. Fiber diameters can be measured with a random uncertainty of 40 nm and a systematic error estimated to be 40 nm.
[Contact: Steve Mechels, (303) 497-5409]

Mechels, S., and Young, M., **Video Microscope with Submicrometer Resolution**, Applied Optics, Vol. 30, No. 16, pp. 2202-2211 (1 June 1991).

We have constructed and evaluated a video micro-

scope with a 150 x 150 μm field of view for performing optical fiber geometry measurements. The microscope consists of a frame-transfer video camera, condensing and filtering optics, a 40X, 0.65 NA microscope objective, and frame digitizing electronics. Using simple digital algorithms, we measure distance with a random uncertainty of about 70 nm across the full field of view, but width measurements suffer from a systematic error between 0.1 and 0.2 μm.
[Contact: Steven Mechels, (303) 497-3223]

Optical Fiber Sensors

Deeter, M.N., Rose, A.H., Day, G. W., and Samuelson, S., **Sensitivity Limits to Ferrimagnetic Faraday Effect Magnetic Field Sensors**, Journal of Applied Physics, Vol. 70, No. 10, pp. 6407-6409 (15 November 1991).

Magnetic field sensors based on the Faraday effect in bulk ferrimagnetic iron garnets exhibit many desirable characteristics, including high sensitivity and a large bandwidth. In general, the sensitivity of these sensors is a function of both the crystal geometry and composition. The geometrical dependence of the sensitivity in nonellipsoidal crystals, such as cylinders, is complicated by their spatially nonuniform demagnetizing factors. We compare sensitivity data obtained from a variety of cylindrical iron garnet samples with two models which predict the effective demagnetizing factor N_{eff} as a function of the length-to-diameter ratio. With respect to composition, we present experimental results of sensitivity versus diamagnetic substitution in the iron garnet series $Y_3Fe_{5-x}Ga_xO_{12}$. As expected, the sensitivity rises sharply as x approaches the compositional compensation point.
[Contact: Merritt N. Deeter, (303) 497-5400]

Rose, A.H., and Day, G.W., **Optical Fiber Voltage Sensors for Broad Temperature Ranges**, Proceedings of SPIE (The International Society for Optical Engineering, P.O. Box 10, Bellingham, Washington 98227-0010), Fiber Optic Components and Reliability, Vol. 1580, pp. 95-103 (1991).

In this paper, we describe the development of an optical fiber ac voltage sensor for aircraft and spacecraft applications. Among the most difficult specifications to meet for this application is a temperature stability of ±1% from -65 °C to +125 °C. This stability requires a careful selection of materials, components, and optical configuration with further compensation using an optical fiber temperature sensor located near the sensing element. The sensor is a polarimetric design, based on the linear electrooptic effect in bulk bismuth germanate ($Bi_4Ge_3O_{12}$). The temperature sensor is also polarimetric, based on the temperature dependence of the birefringence of bulk SiO_2. The temperature sensor output is used to automatically adjust the calibration of the instruments.
[Contact: Allen H. Rose, (303) 497-5599]

Williams, P.A., Clark, N.A., Blanca Ros, M., Vohra, R.T., Walba, D. M., and Wand, M. D., **Large Electroclinic Effect in New Liquid Crystal Material**, Proceedings of the Third International Conference on Ferroelectric Liquid Crystals, Boulder, Colorado, June 23-28, 1991, Vol. 121, pp. 143-146.

We report a new liquid crystal material (W317) which has an unusually large electroclinic effect in a phase tentatively identified as the smectic A. We show electroclinic tilt angles as large as 21°, and measurable tilt angles over a 40 °C temperature range.
[Contact: Paul A. Williams, (303) 497-3805]

Williams, P.A., Rose, A.H., Day, G.W., Milner, T.E., and Deeter, M.N., **Temperature Dependence of the Verdet Constant in Several Diamagnetic Glasses**, Applied Optics, Vol. 30, No. 10, pp. 1176-1178 (1 April 1991).

We report measurements of the temperature dependence of the Verdet constant of SiO_2, SF-57, and BK-7 glasses. In each case, the Verdet constant increases with temperature by the order of 1 part in 10^4/K over the range from room temperature to 150 °C. The results for each glass are within 3 to 20% of estimates obtained using the Becquerel formula with published data for dispersion and the change in index of refraction with temperature.
[Contact: Paul A. Williams, (303) 497-3287]

Electro-Optic Metrology

Boisrobert, C.Y., Franzen, D.L., Danielson, B.L., and Christensen, D.H., **Low Coherence Optical Reflectometry of Laser Diode Waveguides**, Proceedings of SPIE (The International Society for Optical Engineering, P.O. Box 10, Bellingham, Washington 98227-0010), Optical Technology for Signal Processing, Vol. 1474, pp. 285-290 (1991).

Laser diode waveguides are probed using low-coherence optical reflectometry. Reflections from the launch optics, front facet, and rear facet are located with a resolution of approximately 10 µm. Diodes mounted in pigtailed packages and on chip carriers have been studied.
[Contact: Christensen Y. Boisrobert, (303) 497-5052]

Gallawa, R.L., Goyal, I.C., and Ghatak, A.K., **Optical Waveguide Analysis Using Modified Airy Functions,** Fiber and Integrated Optics, Vol. 10, pp. 1-10 (1991).

We review a little-used but powerful method of solving the scalar wave equation. It uses a modification of the well-known Airy functions, which are easily calculated on desktop computers. The techniques are reminiscent of the WKBJ methodology (WKBJ refers to the initials of four independent workers, Wentzel, Kramers, Brillouin, and Jeffrey, who first used the approximation procedure to solve the Schroedinger wave equation in one dimension), but the solution, although approximate, is much more useful than the traditional WKBJ solution and can be used with almost as much ease. The method is extremely powerful but, to our knowledge, is not used in the optics community. It is useful in analyzing integrated optical waveguide components.
[Contact: Robert L. Gallawa, (303) 497-3761]

Ghatak, A.K., Gallawa, R.L., and Goyal, I.C., **Modified Airy Function and WKB Solutions to the Wave Equation,** NIST Monograph 176 (November 1991).

The purpose of this monograph is to revisit a basic equation of mathematical physics, $d^2\Psi/dx^2 + \Gamma^2(x)\Psi(x) = 0$, and to give approximate solutions based on the WKB method (WKB refers to the initials of three independent workers -- Wentzel, Kramers, Brillouin -- who first used the approximation procedure to solve the Schroedinger wave equation in one dimension) and on a modification of the Airy function. All of the examples used to illustrate the methods are based on optical waveguides and quantum mechanical problems. We hope that this monograph will prove to be tutorial, giving insight and understanding to the use of Airy functions in addressing the scalar-wave equation.
[Contact: Robert L. Gallawa, (303) 497-3761]

Goyal, I.C., Gallawa, R.L., and Ghatak, A.K., **An Approximate Solution to the Scalar Wave Equation for Optical Waveguides,** Applied Optics, Vol. 30, No. 21, pp. 2985-2989 (20 July 1991).

We consider an approximate solution to the one-dimensional scalar wave equation appropriate to the planar optical waveguides often encountered in practice. The refractive index profile may be arbitrary. The method described here is more accurate and useful than the WKB method, which has often been applied to problems of this type, as unlike the WKB method, this method is valid even at turning points (WKB refers to the initials of three independent workers -- Wentzel, Kramers, Brillouin -- who first used the approximation procedure to solve the Schroedinger wave equation in one dimension). The fields and the propagation constants for the lowest order modes for two profiles are calculated and compared with the exact solution.
[Contact: Robert L. Gallawa, (303) 497-3761]

Grossman, E.N., Sauvageau, J.E., and McDonald, D.G., **Lithographic Spiral Antennas at Short Wavelengths,** Applied Physics Letters, Vol. 59, No. 25, pp. 3225-3227 (16 December 1991).

We have extended the high efficiency of lithographic antennas to mid-infrared wavelengths. Pattern measurements made at 9.5-µm wavelength on a 65°, self-complementary, spiral antenna exhibit a ratio of response to orthogonal linear polarizations of 1.35 dB, a beamwidth of 85° (3 dB full width), a directivity of 8.2 dB, and surprisingly, a close resemblance to the theoretical pattern for a 65° spiral in free space. Direct detection measurements made with an ambient temperature blackbody source yield an antenna efficiency of 52 ± 7%, when corrected for incomplete filling of the antenna beam by the source, at a mean effective wavelength of 19 µm.
[Contact: Erich N. Grossman, (303) 497-5102]

Obarski, G.E., **Lambdameter for Accurate Stability Measurements of Optical Transmitters,** Proceedings of SPIE (The International Society for Optical Engineering, P.O. Box 10, Bellingham, Washington 98227-0010), Laser Testing and Reliability, Vol. 1620, pp. 41-48 (1991).

Very wavelength-stable, single-mode laser diodes will play an important role in near-future optical fiber

communications systems. Two such applications are sources for dense wavelength multiplexing and local oscillators in coherent systems. To accurately measure wavelength of 1.3- and 1.5-μm single-mode sources, we developed a lambdameter that can also be used in the near IR and red regions of the spectrum. Wavelength accuracy and resolution are ≈0.1 parts per million at the 0.63-μm HeNe laser emission line. They were measured by comparing each of two adjacent modes of a HeNe laser, frequency-stabilized by a polarization technique, with a single mode from a second frequency-stabilized HeNe laser. We also verified the wavelength of the reference laser to 1 part-per-million accuracy by comparing it with the 1.52-μm HeNe laser emission line. The uncertainty in wavelength of the 1.52-μm HeNe laser is limited to the width of the Doppler gain curve whose peak is known within 0.2 parts per million. We describe our lambdameter and the performance of its reference laser as a wavelength transfer standard. Measurements on a commercially packaged 1.52-μm DFB-laser diode transmitter show that its wavelength fluctuates by at least 1 part per million during normal changes in room temperature.
[Contact: Gregory E. Obarski, (303) 497-5747]

Sanford, N.A., Malone, K.J., Larson, D.R., and Hickernell, R.K., **Y-Branch Waveguide Glass Laser and Amplifier**, Optics Letters, Vol. 16, No. 15, pp. 1168-1170 (August 1, 1991).

A Y-branch channel waveguide laser operating near 1057 nm was fabricated in Nd-doped silicate glass by means of electric-field-assisted ion exchange. The overall length was 24 mm. Optical pumping was performed with a continuous wave Ti:sapphire laser. Mirrors were bonded directly to the polished waveguide facets. Using a 4%-transmitting output coupler, the slope efficiency was 5.1%; threshold was reached at 26-mW absorbed pump power. When operated as a single-pass Y-branch amplifier, the small-signal gain was 0.034 dB/mW. The 3-dB splitting loss of the Y-branch structure was overcome when the absorbed pump power was approximately 85 mW.
[Contact: Norman A. Sanford, (303) 497-5239]

Schlager, J.B., Kawanishi, S., and Saruwatari, M., **Dual Wavelength Pulse Generation Using a Mode-Locked Erbium-Doped Fiber Ring Laser**, Electronics Letters, Vol. 27, No. 22, pp. 2072-2073 (24 October 1991).

Dual pulses, each with durations as short as 2 ps and different peak wavelengths, were concurrently produced with an actively mode-locked, erbium-doped fiber ring laser made in part with birefringent polarization-maintaining fiber. Peak-wavelength separation was proportional to the percentage of cavity having properly aligned birefringent fiber.
[Contact: John B. Schlager, (303) 497-3542]

Veasey, D.L., Hickernell, R.K., Larson, D.R., and Batchman, T.E., **Waveguide Polarizers With Hydrogenated Amorphous Silicon Claddings**, Applied Optics, Vol. 16, No. 10, pp. 717-719 (May 15, 1991).

We have fabricated TE- and TM-pass waveguide polarizers with polarization extinction ratios of 42 and 35 dB, respectively. The devices were fabricated by the growth of hydrogenated amorphous silicon claddings on K^+-Na^+ ion-exchanged channel waveguides in glass. Cladding thicknesses were accurately tuned to permit optimum coupling of either a TE or TM mode to the cladding. We have also demonstrated that waveguide losses of at least 760 dB/cm can be measured using a photothermal deflection technique.
[Contact: David L. Veasey, (303) 497-3439]

Veasey, D.L., Larson, D.R., and Batchman, T.E., **In-Situ Optimization of Coupling to Semiconductor Claddings from Dielectric Waveguides**, Journal of Applied Physics, Vol. 68, No. 7, pp. 3753-3755 (1 October 1990).

We have experimentally verified the periodic dependence of coupling between lossless modes of dielectric waveguides and lossy modes supported by semiconductor waveguide claddings as a function of cladding thickness. Results were obtained by the in-situ monitoring of attenuation during the growth and etching of hydrogenated amorphous silicon on polarization-preserving, D-shaped, optical fiber. Strong correlation exists between theoretically predicted and experimental results for both TE and TM polarizations. The attenuation-monitoring technique allows for precise control of waveguide-cladding characteristics so that clad-waveguide devices, such as polarizers and detectors, can be optimized for better performance.
[Contact: David L. Veasey, (303) 497-3439]

Complex System Testing

Stenbakken, G.N., and Souders, T.M., **Linear Error Modeling of Analog and Mixed-Signal Devices,** Proceedings of the 1991 International Test Conference, Nashville, Tennessee, October 26-30, 1991, pp. 573-581.

Techniques are presented for developing linear error models for analog and mixed-signal devices. Methods for choosing parameters and assuring the models are complete and well-conditioned are included. Once established, the models can be used in a comprehensive approach for optimizing the testing of the subject devices.
[Contact: Gerard N. Stenbakken, (301) 975-2440]

Other Signal Topics

Danielson, B.L., and Boisrobert, C.Y., **Absolute Optical Ranging Using Low Coherence Interferometry,** Applied Optics, Vol. 30, No. 21, pp. 2975-2979 (20 July 1991).

We describe a method for measuring submicrometer distances with an asymmetric fiber Michelson interferometer having an LED as a source of radiation. By measuring the phase slope of the Fourier components in the frequency domain, it is possible to locate the position of reflections with nanometer precision even in the presence of sample dispersion. The method is compatible with time-domain sampling at the Nyquist rate which ensures efficiency in data acquisition and processing.
[Contact: Bruce L. Danielson, (303) 497-5620]

Grossman, E.N., Sauvageau, J.E., and McDonald, D.G., **Lithographic Spiral Antennas at Short Wavelengths,** Applied Physics Letters, Vol. 59, No. 25, pp. 3225-3227 (16 December 1991).

We have extended the high efficiency of lithographic antennas to mid-infrared wavelengths. Pattern measurements made at 9.5-μm wavelength on a 65°, self-complementary, spiral antenna exhibit a ratio of response to orthogonal linear polarizations of 1.35 dB, a beamwidth of 85° (3 dB full width), a directivity of 8.2 dB, and surprisingly, a close resemblance to the theoretical pattern for a 65° spiral in free space. Direct detection measurements made with an ambient temperature blackbody source yield an antenna efficiency of 52 ± 7%, when corrected for incomplete filling of the antenna beam by the source, at a mean effective wavelength of 19 μm.
[Contact: Erich N. Grossman, (303) 497-5102]

Ma, M.T., and Adams, J.W., **Phase Characteristics and Time Responses of Unknown Linear Systems Determined from Measured CW Amplitude Data** [original title: Determination of Phase Characteristics and Time Responses of Unknown Linear Systems Based on Measured cw Amplitude Data], NIST Technical Note 1349 (November 1991). [A condensed version, **System Response to Pulsed Excitations Estimated From Measurement of cw Amplitudes,** will be published in the Record of the 1992 International Symposium on Electromagnetic Compatibility, Beijing, China, May 25-27, 1992.]

An alternative technique is described for calculating the complete time and frequency characteristics of an unknown linear system from the measured amplitude response to continuous-wave (cw) excitations by assuming that the system transfer function is minimum phase. The time-response level so determined shows that the susceptibility of the system to damage by pulsed excitation is the greatest during the initial period of excitation. Other possible time responses, when the actual system transfer function is non-minimum phase, are also identified and analyzed.
[Contact: Mark T. Ma, (303) 497-3800]

ELECTRICAL SYSTEMS

Power Systems Metrology

Anderson, W.E., Editor, **Research for Electric Energy Systems - An Annual Report,** NISTIR 4691 (December 1990).

This report documents the technical progress in the four investigations which make up the project "Support of Research Projects for Electrical Energy Systems," Department of Energy Task Order Number 137, funded by the U.S. Department of Energy and performed by the Electricity Division of the National Institute of Standards and Technology (NIST). The first investigation is concerned with the measurement of magnetic fields in support of epidemiological and in-vitro studies of biological field effects. NIST cohosted a workshop on exposure and biological parameters that should be considered during in-vitro

studies with extremely low-frequency magnetic and electric fields. Additionally, equations were developed to predict the magnetic field in a parallel-plate magnetic-field exposure system. An IEEE standard prepared at NIST on measuring dc electric fields and ion-related parameters was approved and published. Various site visits were made to characterize the electric and magnetic fields in biological exposure systems. The second investigation is concerned with two different activities: the detection of trace levels of S_2F_{10} in SF_6 and the development of an improved stochastic analyzer for pulsating phenomena (SAPP). The detection of S_2F_{10} in the presence of SF_6 using mass-spectrometric detection coupled to a gas chromatograph is difficult because of the similar mass spectra. Enrichment techniques, capable of sub parts per billion detection in the case where the background gas is not SF_6, are unsuitable for this application. A technique is described that enables the detection of S_2F_{10} in gaseous SF_6 down to the parts per billion level using a modified gas chromatograph-mass spectrometer. The SAPP has been improved to allow direct real-time measurements of conditional pulse-amplitude distributions of higher order than was previously possible. The new system was applied to an investigation of the stochastic behavior of negative corona (Trichel pulses) and the effect of a dielectric barrier on these discharges. The third investigation is concerned with breakdown and prebreakdown phenomena in liquid dielectrics. The activity reported here was a study of negative streamers preceding electric breakdown in hexanes. Using the image-preserving optical delay, the growth of the streamers associated with partial discharges at a point cathode are photographed at high magnification. Simultaneous discharge current measurements enables a detailed description of the temporal and spatial development of streamers and provide a basis for the evaluation of models for the initiation of negative streamers. The last investigation is concerned with the evaluation and improvement of methods for measuring fast transients in electrical power systems such as might be associated with an electromagnetic impulse. The new draft of IEC-60 recommends the use of an independent reference measurement system to verify the performance of the impulse voltage measuring system under test. A compact resistive divider, NIST4, was designed for this purpose. It is anticipated that this divider, together with some Kerr electro-optical devices, will be used as the reference system at NIST. The design details of NIST 4 and its measurement capabilities are presented.
[Contact: William E. Anderson, (301) 975-2432]

Fenimore, C., and Martzloff, F.D., **Validating Surge Test Standards by Field Experience: High-Energy Tests and Varistor Performance**, Conference Record of the 1990 IEEE Industry Applications Society Annual Meeting, Seattle, Washington, October 7-12, 1990, pp. 1968-1974 (1990).

New, high-energy surge tests are emerging in IEEE and IEC standards. Field experience offers a valuable criterion for validating or invalidating proposed standards. A proposal under consideration by the IEC involves so much energy that a varistor of the voltage rating commonly used in protecting load equipment, if subjected to this test, would almost certainly fail. Yet, reported varistor failure rates do not reflect such a situation. Thus, a re-examination of the premises that led to the proposed test specifications appears necessary. Proposals for high-energy tests as additional waveforms in the new version of IEEE C62.41, on the other hand, lead to current and energy levels that do not place typical varistors in immediate jeopardy. Thus, they appear more consistent with field experience.
[Contact: Charles Fenimore, (301) 975-2428]

FitzPatrick, G.J., and Lagnese, J.E., **Determination of Kerr Cell Parameters with Comparative Digitizer Measurements**, Proceedings of the IEEE International Symposium on Digital Techniques in High-Voltage Measurements, Toronto, Ontario, Canada, October 28-30, 1991, pp. 5-29 to 5-33 (1991).

Kerr cell measurement systems consist of polarimetric devices that modulate a beam of light according to the voltage applied to them. The output consists of a series of intensity oscillations or "fringes." Calibration of Kerr cells have been performed in the past through simultaneous measurements of the Kerr cell and voltage divider outputs using analog oscilloscopes. The evaluation of the Kerr cell constant was then made by comparison of the peak voltages as measured by the two systems. Digitized data are ideal for the application of curve-fitting techniques and are now used for the evaluation of the Kerr parameters (or alternatively, for the determination of the ratio of the voltage divider). The fitting techniques utilize the entire waveforms rather than comparing them at peak voltage only. This paper describes the application of

curve-fitting techniques to digitized waveforms for the evaluation of the Kerr cell constants. The results for Kerr cells used to cover the range from 10 kV to 300 kV are presented. Cell constants for the same cell geometry but with different Kerr liquids are also reported. The uncertainties of the evaluated Kerr cell parameters and their dependence on fringe number are discussed. The effects on the evaluated cell constants produced by segmenting the digitized Kerr waveforms are also examined.
[Contact: Gerald J. FitzPatrick, (301) 975-2737]

Martzloff, F.D., **A Standard for the 90s: IEEE C62.41 Surges Ahead** [original title: IEEE Guide on Surge Voltages Upgraded to Recommended Practice], Compliance Engineering, Vol. 8, No. 5, pp. 27-ff (Fall 1991).

After ten years of use as a guide, a revision has been completed and published as an IEEE Recommended Practice: Surge Voltages in Low-Voltage AC Power Circuits. This article appears in a trade magazine circulated to writers, users, and enforcers of standards on electromagnetic compatibility in order to give them a preview of the forthcoming IEEE document.
[Contact: Francois D. Martzloff, (301) 975-2409]

Martzloff, F.D., and Lai, J.S., **Cascading Surge-Protective Devices: Coordination Versus the IEC 664 Staircase**, Proceedings of the First International Conference on Power Quality: End-Use Applications and Perspectives, Gif-sur-Yvette, Paris, France, October 15-18, 1991, pp. 191-198.

Cascading two or more surge-protective devices located, respectively, at the service entrance of a building and near the sensitive equipment is intended to ensure that each device shares the surge stress in a manner commensurate with its rating to achieve reliable protection of equipment against the surges impinging from the utility supply, as well as internally generated surges. However, depending upon the relative clamping voltages of the two devices, their separation distance, and the waveform of the impinging surge, coordination may or may not be effective. The paper reports computations confirmed by measurements of the energy deposited in the devices for combination of these three parameters.
[Contact: Francois D. Martzloff, (301) 975-2409]

Martzloff, F.D., and Mendes, A., **Standards: Transitional Aspects**, Proceedings of the First International Conference on Power Quality: End-Use Applications and Perspectives, Gif-sur-Yvette, Paris, France, October 15-18, 1991, pp. 31-34.

Mass production of electrical and electronic equipment for the world market requires a system of standards of worldwide applicability. The development of such standards is a complex task, involving various national and international organizations. This paper presents a review of the standards-writing process, in particular, the area of power quality.
[Contact: Francois D. Martzloff, (301) 975-2409]

McComb, T.R., and Lagnese, J.E., **Calculating the Parameters of Full Lightning Impulses Using Model-Based Curve Fitting**, IEEE Transactions on Power Delivery, Vol. 6, No. 4, pp. 1386-1394 (October 1991).

A brief review is presented of the techniques used for the evaluation of the parameters of high-voltage impulses and the problems encountered. The determination of the best smooth curve through oscillations on a high-voltage impulse is the major problem limiting the automatic processing of digital records of impulses. Nonlinear regression, based on simple models, is applied to the analysis of simulated and experimental data of full lightning impulses. Results of model fitting to four different groups of impulses are presented and compared with some other methods. Plans for the extension of this work are outlined.
[Contact: Terry R. McComb, (301) 975-3954]

Misakian, M., **In Vitro Exposure Parameters with Linearly and Circularly Polarized ELF Magnetic Fields**, Bioelectromagnetics, Vol. 12, No. 6, pp. 377-381 (October 1991).

A comparison is made of induced current densities, electric fields, and rate of energy deposition during in-vitro studies with linearly and circularly polarized extremely low frequency (ELF) magnetic fields.
[Contact: Martin Misakian, (301) 975-2426]

Olthoff, J.K., Van Brunt, R.J., Wang, H-X., Moore, J.H., and Tossell, J.A., **Total Cross Sections for Electron Scattering and Attachment for SF_6 and Its Electrical-Discharge By-Products** [original title: Absolute Total Electron Scattering and Dissociative Attachment Cross Sections of By-Products from

Electrical Discharges in SF_6], Gaseous Dielectrics VI, L. G. Christophorou and I. Sauers, Eds. (Plenum Press, New York, 1991), pp. 19-25. [Proceedings of the Sixth International Symposium on Gaseous Dielectrics, Knoxville, Tennessee, September 23-27, 1990.]

Using an electron transmission spectrometer, the absolute total dissociative attachment cross sections of SF_6 and of its decomposition products have been measured as a function of electron energy over the range of 0.2 eV to 5.0 eV, and absolute total electron scattering cross sections have been measured from 0.2 eV to 12 eV. These results are presented along with previous data where available.
[Contact: James K. Olthoff, (301) 975-2431]

Sauers, I., Harman, G., Olthoff, J.K., and Van Brunt, R.J., **S_2F_{10} Formation by Electrical Discharges in SF_6: Comparison of Spark and Corona**, Gaseous Dielectrics VI, L. G. Christophorou and I. Sauers, Eds. (Plenum Press, New York, 1991), pp. 553-561. [Proceedings of the Sixth International Symposium on Gaseous Dielectrics, Knoxville, Tennessee, September 23-27, 1990.]

Among the SF_6 by-products of electrical discharges that have been investigated, S_2F_{10} is probably the least understood (physical, chemical, and biological properties) and the most toxic. Its production in electrical discharges has been controversial since the presence of this chemical has been reported by only a few groups. We report on the yields of S_2F_{10} in two types of discharges: spark and corona. The S_2F_{10} yields for corona and spark were 2.4 μmol/C and 0.04 to 0.37 nmol/J, respectively, for experiments where the water content was low. For both types of discharges, we have found that S_2F_{10} formation is dependent on the presence of moisture. For corona discharges, model calculations based on known sulfur-fluorine chemistry are shown to yield reasonable agreement with experimental data. We show that S_2F_{10} was formed in electrical discharges expected to be found in compressed-gas insulated equipment, and address such factors as effects of moisture and surface conditions.
[Contact: James K. Olthoff, (301) 975-2425]

Turgel, R.S., **Electricity in the Year 2000**, Proceedings of the IEEE Technical Activities Board (TAB) Symposium, Mexico City, Mexico, October 3, 1991, pp. 1-5.

Demand for electricity is predicted to rise at a rate higher than that of the creation of new generating capacity. Projections suggest that a shortfall of 100 million kilowatts may be reached by the year 2000. Various measures to alleviate the projected shortfall are discussed.
[Contact: Raymond S. Turgel, (301) 975-2420]

Van Brunt, R.J., **S_2F_{10}: A Clarification**, Electrical Review, Vol. 224, No. 22, p. 10 (November 15, 1991).

"SF_6 product '3,000 times deadlier than phosgene'" (Electrical Review, 20 September-3 October) reports, among other topics, results obtained by researchers at the National Institute of Standards and Technology. This letter to the editor addresses some misstatements that occur in the article, referring to the NIST work.
[Contact: Richard J. Van Brunt, (301) 975-2425]

Van Brunt, R.J., **Stochastic Properties of Partial-Discharge Phenomena**, IEEE Transactions on Electrical Insulation, Vol. 26, No. 5, pp. 902-948 (October 1991).

Prebreakdown pulsating partial-discharge (P-D) phenomena that occur in dielectric media are inherently complex stochastic processes that exhibit significant statistical variability in such properties as pulse amplitude, shape, and time of occurrence. Previously published work concerned with the theory and measurement of the stochastic behavior of PDs is reviewed. The types of P-D phenomena considered in this review include ac- and dc-generated electron avalanches, pulsating positive and negative corona in gases, and partial discharges that occur in liquid media and in the presence of solid dielectric surfaces. The basic physical mechanism distributions for pulse occurrence times and pulse amplitudes are discussed. Consideration is also given to special problems associated with the measurement and interpretation of data on the various statistical properties of P-D phenomena.
[Contact: Richard J. Van Brunt, (301) 975-2425]

Van Brunt, R.J., and Cernyar, E.W., **Influence of Phase-to-Phase Memory Propagation on the Stochastic Behavior of AC-Generated Partial Discharg-**

es, 1991 Annual Report, Conference on Electrical Insulation and Dielectric Phenomena (CEIDP), Knoxville, Tennessee, October 20-23, 1991, pp. 589-596.

From measurements of phase-restricted conditional partial-discharge amplitude and phase-of-occurrence distributions performed for the first time, it has been possible to observe the influence of phase-to-phase memory propagation on the stochastic behavior of partial discharges generated by applying an ac voltage to a point electrode in contact with a solid dielectric surface. "Memory" associated with charge deposited on the dielectric surface by preceding discharge events is found to have a significant effect in determining the most probable phase-of-occurrence and amplitudes of subsequent partial-discharge pulses. It is found, for example, that the larger amount of charge deposited during partial-discharge activity on one-half cycle, the sooner will be the time (or phase) of occurrence of the partial discharges on the next half cycle. The observed memory effect is expected from consideration of the surface charging dynamics and must be considered in any attempt to interpret results of phase-resolved partial-discharge measurements.
[Contact: Richard J. Van Brunt, (301) 975-2425]

Van Brunt, R.J., and Kulkarni, S., **Influence of Memory on the Statistics of Pulsating Corona**, Gaseous Dielectrics VI, L. G. Christophorou and I. Sauers, Eds. (Plenum Press, New York, 1991), pp. 383-389. [Proceedings of the Sixth International Symposium on Gaseous Dielectrics, Knoxville, Tennessee, September 23-27, 1990.]

In order to develop a theory that accounts for observed pulse-time separation and pulse-amplitude distributions for pulsating corona discharges in gases, it is necessary to consider the effects of residuals from prior discharge pulses, such as ion space charge and metastables, on the development of subsequent pulses. Such "memory effects" are shown here to be significant in controlling the statistics of Trichel-pulse corona in electro-negative gases. The memory effects are quantitatively assessed from a direct measurement of a set of conditional pulse-amplitude and pulse-time-separation distributions. The effectiveness of this method in providing a more complete description and better understanding of the stochastic behavior of corona is illustrated here for the case of self-sustained Trichel pulse in a neon-oxygen gas mixture. The amplitude and time of initiation of any discharge pulse is found to be strongly dependent on the amplitude of the previous pulse, as well as on the time that has elapsed since that pulse occurred. Memory is found to extend back beyond the most recent pulse so that the process is distinctly non-Markovian.
[Contact: Richard J. Van Brunt, (301) 975-2425]

Magnetic Materials and Measurements

Chen, D-X., Brug, J.A., and Goldfarb, R.B., **Demagnetizing Factors for Cylinders**, IEEE Transactions on Magnetics, Vol. 27, No. 4, pp. 3601-3619 (July 1991).

We have calculated fluxmetric and magnetometric demagnetizing factors N_f and N_m for cylinders as functions of susceptibility χ and the ratio of length to diameter γ. For $\chi = 0$, applicable to weakly magnetic or saturated ferromagnetic materials, N_f and N_m are calculated using a formula for the mutual inductance of concentric coaxial thin solenoids. N_f for $-1 \leq \chi < \infty$ and N_m for $\chi \rightarrow \infty$ when $\gamma \geq 10$ are calculated using a one-dimensional model. For $1 \leq \gamma \leq 10$, an important range for magnetometer measurements, N_m for both $\chi \rightarrow \infty$ and $\chi < 0$ are obtained by extrapolation from data at larger γ. The case $\chi < 0$ is applicable to conductors and superconductors. General rules for demagnetizing factors are discussed.
[Contact: Ronald B. Goldfarb, (303) 497-3650]

Moreland, J., and Rice, P., **Imaging Magnetic Bit Patterns Using a Scanning Tunneling Microscope with a Flexible Tip**, Proceedings of the Materials Research Society Symposium, Anaheim, California, April 30-May 3, 1991, Vol. 232, pp. 141-146.

Tunneling stabilized magnetic force microscopy (TSMFM) is a variant of scanning tunneling microscopy (STM) where the usual rigid STM tip is replaced with a flexible magnetic tip. This method contrasts with other magnetic force microscopes based on optical detection of cantilever deflection due to magnetic forces. Instead, the position of the flexible tunneling tip depends on both topography and magnetic forces acting on the end of the tip. The z-motion of the piezoelectric translator flexes the tip to balance the magnetic force so that the end of the tip remains a fixed tunneling distance from the sample surface. We present TSMFM images showing the recorded bit patterns of hard disk, floppy disk, and

tape surfaces. The images were taken in air using free-standing, thin-film (about 1-μm-thick) Fe and Ni flexible STM tips. The image resolution of TSMFM is routinely submicrometer. We conclude that this simple modification of STM will be a valuable diagnostic tool in the magnetic recording industry.
[Contact: John Moreland, (303) 497-3641]

Superconductors

Ekin, J.W., **Effect of Cable and Strand Twist-Pitch Coincidence on the Critical Current of Flat, Coreless Superconductor Cables,** Applied Physics Letters, Vol. 59, No. 20, pp. 2615-2617 (11 November 1991).

We present data which indicate that a very simple technique of enhancing the critical current in flat, coreless superconductor cables is to match the cable twist pitch with the strand twist pitch. In this manner, the same group of filaments within each strand are degraded at each successive bend at the cable edges. This coincident-twist method minimizes current transfer among filaments, enhances the slope of the voltage-current characteristic, consistently improves the critical current by about 10% in these tests, and is easy to apply.
[Contact: John W. Ekin, (303) 497-5448]

Goodrich, L.F., **Critical Current Measurement on High T_c Superconductors,** Report of the Third Annual U.S.-Japan Workshop on Semiconductors, Buffalo, New York, September 20-21, 1990, pp. 64-68 (1990).

A passive voltage-current (V-I) simulator has been developed and tested using conventional direct current (dc), lock-in amplifier and pulse current methods. The simulator was designed to generate the extremely nonlinear V-I characteristic of a superconductor. It is intended to be used to test various components of the measurement system, such as instrumentation, measurement method, and data analysis software, to determine the transport critical current (I_c) or critical current density (J_c) of a superconductor. Comparison of the pulse current and the lock-in amplifier methods with the conventional direct current method on the passive simulator is presented. Also, preliminary comparisons of dc and pulse methods using a thin-film YBCO sample are given.
[Contact: Loren F. Goodrich, (303) 497-3143]

Goodrich, L.F., Srivastava, A.N., and Stauffer, T.C., **Simulators of Superconductor Critical Current: Design, Characteristics, and Applications,** Journal of Research of the National Institute of Standards and Technology, Vol. 96, No. 6, pp. 703-724 (November-December 1991).

The superconductor simulator is an electronic circuit that emulates the extremely nonlinear voltage-current characteristic (the basis of a critical-current measurement) of a superconductor along with its other major electrical properties. Three different types of simulators have been constructed: the passive, active, and hybrid simulator. The passive simulator has the fewest circuit components and offers the least amount of versatility, while the active and hybrid simulators offer more versatility and consequently have more components. Design, characteristics, and applications of the superconductor simulator along with a summary of features are presented. These simulators are high-precision instruments, and are thus useful for establishing the integrity of part of a superconductor measurement system. They are potentially useful for testing the measurement method and data acquisition and analysis routines. The 50-A simulator provides critical-current precision of 0.1% at a 1-μV signal. This is significantly higher than the precision of a superconducting standard reference material. The superconductor simulator could significantly benefit superconductor measurement applications that require high-precision quality assurance.
[Contact: Loren F. Goodrich, (303) 497-3143]

Ishida, T., Goldfarb, R.B., Okayasu, S., and Kazumata, Y., **Static and Nonlinear Complex Susceptibility of $YBa_2Cu_3O_7$,** Physica C, Vol. 185-189 (Elsevier Science Publishers B.V., North-Holland, 1991), pp. 2515-2516.

We have investigated the harmonic susceptibility $\chi_n = \chi_{n'} - i\chi_{n''}$ (n = 1,2,3,...) of sintered $YBa_2Cu_3O_7$ in the field of $H_{dc} + H_{ac}\sin\omega t$. $\chi_{1'}$ and $\chi_{1''}$ as functions of temperature depend on both H_{ac} and H_{dc}. Both even and odd χ_n's were detected for nonzero H_{dc}, but only odd harmonics were observed for zero H_{dc}. At constant temperature, χ_n is an even function of H_{dc} for n = odd, while χ_n is an odd function of H_{dc} for n = even. We compared experimental features with the prediction of the critical state model. For comparison, the static susceptibility χ_{dc} of $YBa_2Cu_3O_7$ was examined as a function of temperature. The $\chi_{dc}(T)$

for the sample cooled in small fields is unusual; a negative peak occurs near T_c, which can be explained by intragranular flux depinning upon warming.
[Contact: Ronald B. Goldfarb, (303) 497-3650]

Loughran, R.J., and Goldfarb, R.B., **Anisotropic Weak-Link Properties and Intergranular Lower Critical Field of Grain-Aligned $YBa_2Cu_3O_x$**, Physica C, Vol. 181 (Elsevier Science Publishers B.V., North-Holland, 1991), pp. 138-142.

We studied the weak-link nature of sintered, grain-aligned $YBa_2Cu_3O_x$ using dc magnetization and ac susceptibility. The sample was highly anisotropic for fields applied perpendicular and parallel to the grains' a,b planes. The bulk demagnetizing factor was the same for the two field directions. For fields applied perpendicular to the a,b planes, the magnetization curves show small intergranular coupling losses, and the susceptibility curves show sharp coupling transitions. From ac susceptibility measurements in parallel and perpendicular fields, respectively, the intergranular lower critical fields are no higher than 0.15 kA/m (1.9 Oe) and 0.3 kA/m (3.8 Oe) at 76 K and 0.5 kA/m (6.3 Oe) and 1.3 kA/M (16.3 Oe) at 4 K.
[Contact: Robert J. Loughran, (303) 497-3547]

Moreland, J., Rice, P., Russek, S.E., Jeanneret, B., Roshko, A., Ono, R.H., and Rudman, D.A., **Scanning Tunneling Microscopy of the Surface Morphology of $YBa_2Cu_3O_x$ Thin Films Between 300 K and 76 K**, Applied Physics Letters, Vol. 59, No. 23, pp. 3039-3041 (2 December 1991).

Scanning tunneling microscopy (STM) images of $YBa_2Cu_3O_x$ (YBCO) thin films show different growth habits depending on the deposition method and substrate material. In particular, we present images of YBCO films sputter deposited onto MgO and $SrTiO_3$ and laser ablated onto $LaAlO_3$. Both screw dislocation and ledge growth are observed. The STM morphology of YBCO films sputtered onto MgO substrates is investigated as a function of temperature. We find that at room temperature growth steps have an anomolously large apparent height which decreases with decreasing temperature, approaching the expected value for one unit cell of 1.2 nm at 76 K. Presumably, this phenomenon reflects changes in either the surface tunneling barrier or tunneling density of states upon cooling.
[Contact: John Moreland, (303) 497-3641]

Shi, D., Salem-Sugui, S., Jr., Wang, Z., Goodrich, L.F., Dou, S.X., Liu, H.K., Guo, Y.C., and Sorrell, C.C., **Critical Currents in Silver-Sheathed $(Bi,Pb)_2Sr_2Ca_2Cu_3O_{10-y}$ Superconducting Tapes**, Applied Physics Letters, Vol. 59, No. 24, pp. 3171-3173 (9 December 1991).

Nearly 95 vol% of the 110-K superconducting phase was formed by lead doping in a Bi-Sr-Ca-Cu-O system. The processed 110-K superconducting powders were used to produce long silver-sheathed tapes with a highly textured microstructure by rolling and prolonged sintering. The transport critical-current density was measured at 4.2 K to be 0.7×10^5 A/cm^2 at zero field and 1.6×10^4 A/cm^2 at 12 T for H parallel to the plane defined by the a and b axes. At 77 K, the critical-current density reached a value of $\sim 1 \times 10^4$ A/cm^2 at zero field for H parallel to the plane defined by the a and b axes and gradually decreased to 419 A/cm^2 at 1 T. Excellent grain alignment in the a-b plane led to a greatly improved critical-current density under a magnetic field. The relationship between the transport properties and the microstructure of the tapes is discussed.
[Contact: Loren F. Goodrich, (303) 497-3143]

ELECTROMAGNETIC INTERFERENCE

Conducted

Fenimore, C., and Martzloff, F.D., **Validating Surge Test Standards by Field Experience: High-Energy Tests and Varistor Performance**, Conference Record of the 1990 IEEE Industry Applications Society Annual Meeting, Seattle, Washington, October 7-12, 1990, pp. 1968-1974 (1990).

New, high-energy surge tests are emerging in IEEE and IEC standards. Field experience offers a valuable criterion for validating or invalidating proposed standards. A proposal under consideration by the IEC involves so much energy that a varistor of the voltage rating commonly used in protecting load equipment, if subjected to this test, would almost certainly fail. Yet, reported varistor failure rates do not reflect such a situation. Thus, a re-examination of the premises that led to the proposed test specifications appears necessary. Proposals for high-energy tests as additional waveforms in the new version of IEEE C62.41, on the other hand, lead to current and energy levels that do not place typical varistors in

immediate jeopardy. Thus, they appear more consistent with field experience.
[Contact: Charles Fenimore, (301) 975-2428]

Lai, J-S., and Martzloff, F.D., **Coordinating Cascaded Surge Protection Devices: High-Low Versus Low-High**, Proceedings of the 1991 IEEE Industry Applications Society Annual Meeting, Dearborn, Michigan, September 28-October 4, 1991, Vol. II, pp. 1812-1819.

Cascading surge-protective devices between the service entrance of a building and the place near sensitive equipment within the building are intended to ensure that each device shares the surge stress in optimum manner to achieve reliable protection of equipment against surges impinging from the utility supply. However, depending upon the relative clamping voltages of the two devices, their separation distance, and the waveform of the impinging surges, the coordination may or may not be effective. This paper provides computations with experimental verification of the energy deposited in the devices for a matrix of combinations of these three parameters. Results show effective coordination for some combinations and ineffective for some others, a result that should reconcile contradicting findings reported by different authors making different assumptions. From these results, improved coordination can be developed by application standards writers and system designers.
[Contact: Francois D. Martzloff, (301) 975-2409]

Martzloff, F.D., **A Standard for the 90s: IEEE C62.41 Surges Ahead** [original title: IEEE Guide on Surge Voltages Upgraded to Recommended Practice], Compliance Engineering, Vol. 8, No. 5, pp. 27-ff (Fall 1991).

After ten years of use as a guide, a revision has been completed and published as an IEEE Recommended Practice: Surge Voltages in Low-Voltage AC Power Circuits. This article appears in a trade magazine circulated to writers, users, and enforcers of standards on electromagnetic compatibility, in order to give them a preview of the forthcoming IEEE document.
[Contact: Francois D. Martzloff, (301) 975-2409]

Radiated

Crawford, M.L., and Riddle, B.F., **A Proposed TEM Driven Mode-Stirred Chamber for Large System Radiated EMC/V Testing, 10 kHz to 40 GHz**, Proceedings of the Electromagnetic Compatibility Symposium, Zurich, Switzerland, March 12-14, 1991, pp. 431-437.

This paper describes work in progress at the National Institute of Standards and Technology to develop a single, integrated facility for whole system electromagnetic susceptibility/vulnerability (EMC/V) testing over the frequency range of 10 kHz to 40 GHz. The facility will consist of a large shielded enclosure, 13.1 m by 24.1 m by 38.7 m in size, configured as a TEM transmission line-driven, mode-stirred chamber. The anticipated test volume is 7 m by 16 m by 30 m. TEM test fields are generated in the chamber at frequencies below multimode cutoff. The paper discusses a proposed design, advantages and limitation, the theoretical basis for the concept, and the experimental approach for using such a facility. Results of an evaluation of a 1/10 scale model chamber (1.3 m by 2.4 m by 3.9 m) are given.
[Contact: Myron L. Crawford, (303) 497-5497]

Koepke, G.H., Driver, L.D., Cavcey, K.H., Masterson, K.D., Johnk, R., and Kanda, M., **Standard Spherical Dipole Source**, NIST Technical Note 1351 (December 1991).

This report describes the development of a standard spherical dipole transmitter that operates from 10 to 1000 MHz. The report includes the complete electronic, mechanical, optical, and theoretical details that are necessary to construct this device and predict the electromagnetic fields which are radiated in simple environments.
[Contact: Galen H. Koepke, (303) 497-5766]

Ma, M.T., Larsen, E.B., and Crawford, M.L., **Electromagnetic Fields with Arbitrary Wave Impedances Generated Inside a TEM Cell**, IEEE Transactions on Electromagnetic Compatibility, Vol. 33, No. 4, pp. 358-362 (November 1991).

Standard electromagnetic fields having a wide range of wave impedances can be generated inside a TEM cell for rf susceptibility testing purposes. We propose to achieve this by (a) exciting both ports of the TEM cell with the desired amplitudes and phases, or (b) exciting only one port, as usual, and terminating the other port with an unmatched load impedance. Both theoretical expressions and experimental results are

presented in this paper.
[Contact: Mark T. Ma, (303) 497-3800]

ADDITIONAL INFORMATION

Lists of Publications

DeWeese, M.E., **Metrology for Electromagnetic Technology: A Bibliography of NIST Publications,** NISTIR 3972 (August 1991).

This bibliography lists the publications of the personnel of the Electromagnetic Technology Division of NIST in the period from January 1970 through publication of this report. A few earlier references that are directly related to the present work of the Division are included.
[Contact: Sarabeth Moynihan, (303) 497-3678]

Lyons, R.M., and Gibson, K.A., **A Bibliography of the NIST Electromagnetic Fields Division Publications,** NISTIR 3973 (August 1991).

This bibliography lists publications by the staff of the National Institute of Standards and Technology's Electromagnetic Fields Division for the period from January 1970 through August 1991. Selected earlier publications from the Division's predecessor organizations are included.
[Contact: Kathryn A. Gibson, (303) 497-3132]

Palla, J.C., and Meiselman, B., **Electrical and Electronic Metrology: A Bibliography of NIST Electricity Division's Publications, NIST List of Publications 94** (January 1992).

This bibliography covers publications of the Electricity Division, Center for Electronics and Electrical Engineering, NIST, and of its predecessor sections for the period January 1968 to December 1991. A brief description of the Division's technical program is given in the introduction.
[Contact: Jenny C. Palla, (301) 975-2220]

Walters, E.J., **Semiconductor Measurement Technology, 1990-1991, NIST List of Publications 103** (April 1992) and **Semiconductor Measurement Technology, 1962-1989, NIST List of Publications 72** (March 1990).

The bibliography provides information on technology transfer in the field of microelectronics at NIST for the calendar years 1990 and 1991. Publications from groups specializing in semiconductor electronics are included, along with NIST-wide research now coordinated by the NIST Office of Microelectronics Programs which was established in 1991. Indices by topic area and by author are provided. Earlier reports of work performed during the period from 1962 through December 1989 are provided in NIST List of Publications 72.
[Contact: E. Jane Walters, (301) 975-2050]

New NIST Research Material

NIST has announced the availability of **Research Material 8458**, a well-characterized artificial flaw used as an **artifact standard in eddy current nondestructive evaluation** (NDE). The new Research Material (RM) is the outcome of work carried out by the Electromagnetic Technology Division to address the need for calibration standards for eddy-current NDE, for example, as used to detect fatigue cracks in aircraft structures. The RM flaw is produced in an annealed aluminum alloy block by first indenting the block and then compressively deforming the resulting notch until it is tightly closed. The next operation is to restore a flat finish to the block face, after which the block is heat treated to the original temper. The controlled flaw has been named the "CDF notch," after its inventors (listed on patent application) Thomas E. Capobianco (Electromagnetic Technology Division), William P. Dube (Division 832), and Ken Fizer (Naval Aviation Depot, NAS Norfolk, Virginia).

In the past, the challenge has been to manufacture artificial flaws that closely simulate the mechanical properties of fatigue cracks. Currently used artifacts include electrical-discharge-machined and saw-cut notches, both of which are relatively poor representations of fatigue cracks as their widths are too great. The Division-developed method provides notches that can be made controllably in a variety of geometries, have known dimensions, with widths that are narrow enough to provide an acceptable representation of fatigue cracks.

An NIST Research Material is not certified by NIST, but meets the International Standards Organization definition of "a material or substance one or more properties of which are sufficiently well established to be used in the calibration of an apparatus, the assess-

ment of a measurement method, or for assigning values to materials." The documentation issued with RM 8458 is a "Report of Investigation." Contact: technical information — Fred Fickett, (303) 497-3785; order information — Standard Reference Materials Program, (301) 975-6776.

Continuing Production-Expanded Capability Standard Reference Materials

The Semiconductor Electronics Division announces the continuing production of three thicknesses and the addition of two new thicknesses for the Standard Reference Material (SRM) for **ellipsometrically derived thickness and refractive index of a silicon dioxide film on silicon.** For sale to the public through the NIST Standard Reference Material Program [(301) 975-6776], the following three individual oxide thicknesses continue to be available: 50 nm (SRM 2531), 100 nm (SRM 2532), and 200 nm (SRM 2533). Recently, two new thicknesses, 25 nm (SRM 2534) and a limited number of 14-nm prototypes (SRM 2535), were added to the availability list.

SRMs 2531, 2532, and 2533, originally released as SRM 2530-1, 2530-2, and 2530-3, were developed in response to the industry's need to evaluate the accuracy of ellipsometers and other thin-film thickness-monitoring instruments. The scope of these SRMs has now expanded with the recent issuance of the 25-nm and 14-nm oxide thicknesses so they have application as thickness standards for use in research as well as in semiconductor fabrication production lines.

Each SRM unit, consisting of a 76-mm (3-in) diameter silicon wafer on which a uniform silicon dioxide layer has been grown, is individually measured and certified over a 5-mm diameter area in the center of the wafer for the ellipsometric parameters delta, Δ, and psi, ψ, at the vacuum wavelength $\lambda = 633.0$ nm using the High-Accuracy Ellipsometer built at NIST. Each SRM is also certified for the derived values for the thicknesses and indices of refraction of both layers of a two-layer optical model of an oxide film on a single-crystal silicon substrate.
[Contact: Barbara J. Belzer, (301) 975-2248]

Recently Issued Standard Reference Materials

The Microelectronics Dimensional Metrology Group of the Precision Engineering Division announces the release of two Standard Reference Materials (SRMs) for calibrating optical microscopes used to measure linewidths on photomasks. Each SRM consists of a 63.5 × 63.5 × 1.5 mm (2.5 × 2.5 × 0.060 in) photomask patterned with chromium lines of widths in the range of 0.9 to 10.8 µm. SRM 475, patterned with antireflecting chromium on a quartz substrate, is being reissued after being out of production for almost four years. SRM 476, a new SRM, is patterned with bright chromium on a borosilicate substrate.

In addition to isolated opaque lines on a clear background and isolated clear lines on an opaque background, these SRMs contain opaque line pairs for calibrating the length scale of optical microscopes, adjacent clear and opaque lines of approximately equal widths for setting the line-to-space ratio (contrast) on video image-scanning instruments, and features with 10 approximately equally spaced opaque lines for checking the linearity of measurement systems (e.g., the magnification as a function of position over the field of view).

The certified linewidth and spacing values were determined from measurements made with the NIST automated linewidth measurement system. The uncertainty of the linewidth measurements is 0.081 µm or less for SRM 475 and 0.064 µm or less for SRM 476. The dominant contribution to this uncertainty is the nonvertical geometry of the line edges, and finding a source of photomasks with better edge geometry would lead to considerable improvement in the calibration uncertainty.
[Contact: James Potzick, (301) 975-3481 or Robert Larrabee, (301) 975-2298]

Emerging Technologies in Electronics ... and Their Measurement Needs, Second Edition

This report assesses the principal measurement needs that must be met to improve U.S. competitiveness in emerging technologies within several fields of electronics: semiconductors, superconductors, magnetics, optical fiber communications, optical fiber sensors, lasers, microwaves, video, and electromagnetic compatibility. The report seeks feedback from industry and Government agencies on the assessment. The feedback will guide the development of NIST programs that provide U.S. industry with new documented measurement methods, new national reference

standards to assure the accuracy of those measurement methods, and new reference data for electronic materials. Copies may be obtained by ordering Report No. PB90-188087/AS ($23.00 hard copy, $11.00 microfiche) from the National Technical Information Service, 5285 Port Royal Road, Springfield, VA 22161, (703) 487-4650.

Transfer of Pulse Waveform Measurements Services to NIST, Gaithersburg, MD

The responsibility for the Special Test Services Provided by NIST for pulse waveform measurements has now been officially transferred to the Electricity Division, Electronic Instrumentation and Metrology Group (811.02) in Gaithersburg, MD. These services include:

Test Number	Description of Services
65100S	Impulse Generator Spectrum Amplitude (50 Ohm)
65200S	Fast Repetitive Broadband Pulse Parameters (50 Ohm)
65300S	Network Impulse Response (S_{21}) of Coaxial Networks
65400S	Pulse Time Delay through Coaxial Transmission Lines

Service for test number 65400S is already available; it is anticipated that the equipment and software necessary for bringing the other waveform measurement services on line will also become available by June 30, 1992. Please direct specific technical questions concerning these services to Mr. William L. Gans, (301) 975-2502.

1992/1993 EEEL CALENDAR

October 8, 1992 (Gaithersburg, Maryland)

Ion Implant Users Group Meeting. Topics to be discussed at this NIST-sponsored meeting include Simulation and Modeling (Part 2). An afternoon tour of the Semiconductor Electronics Division, SED's Semiconductor Processing Research Facility, the Secondary Ion Mass Spectrometry Facility, and the Reactor's Cold Neutron Research Facility is planned.
[Contact: John Albers, (301) 975-2075]

November 9-10, 1992 (Austin, Texas)

Workshop on Process Control Measurements for Advanced IC Manufacturing. In conjunction with SEMICON Southwest, the workshop, cosponsored by ASTM, JEIDA, JESSI, NIST, SEMATECH, SEMI, and SRC, will begin with overviews of the status of process control measurements in silicon device fabrication. Working sessions will consider the critical process control measurement issues in the following areas: film deposition, contamination, implant, etching, oxidation/diffusion, lithography, and materials. Standards development meetings will be held concurrently by ASTM Committee F-1 on Electronics and a selected number of SEMI Standards committees.
[Contact Robert I. Scace, (301) 975-4400]

February 2-4, 1993 (Austin, Texas)

9th Annual IEEE Semiconductor, Thermal Measurement and Management Symposium (SEMI-THERM). Sponsored by IEEE CHMT and NIST, SEMI-THERM is the premier forum for the exchange of information on thermal management of electronics systems between the academic and industrial communities. The program will address the following topics: analytical and computational modeling; measurement techniques including temperature, fluid flow, and thermal-mechanical properties; and thermal reliability screening and testing.
[Contact: David Blackburn, (301) 975-2053]

EEEL SPONSORS

National Institute of Standards and Technology
U.S. Air Force
  McClelland Air Force Base; Newark Air Force Station; Rome Air Development Center; Space & Missile Organization; Wright-Patterson Air Force Base; SAF/FMBMB, Pentagon
U.S. Army
  Dugway Proving Ground; Fort Belvoir; Fort Huachuca; Harry Diamond Laboratory; Strategic Defense Command; AVRADCOM (Aviation)
Department of Commerce
  NOAA; Census
Department of Defense
  Advanced Research Projects Agency; Combined Army/Navy/Air Force (CCG); National Security

Agency; Oak Ridge National Laboratory
Department of Energy
Energy Systems Research; Fusion Energy; Basic Energy Sciences; High Energy & Nuclear Physics
Department of Justice
Law Enforcement Assistance Administration; FBI
U.S. Navy
Naval Sea Systems Command; Weapons Support Center/Crane; Office of Naval Research; Naval Air Systems Command; Naval Air Engineering Center; Naval Research Laboratory; Naval Aviation Depot; Naval Command, Control, and Ocean Surveillance Center, RDT&E Center; Naval Air Test Center; Naval Surface Warfare Center
National Aeronautics and Space Administration
NASA Headquarters; Goddard Space Flight Center; Lewis Research Center
Nuclear Regulatory Commission
Department of Transportation
National Highway Traffic Safety Administration
MIMIC Consortium
Various Federal Government Agencies

NIST-114A (REV. 3-90)

U.S. DEPARTMENT OF COMMERCE
NATIONAL INSTITUTE OF STANDARDS AND TECHNOLOGY

BIBLIOGRAPHIC DATA SHEET

1. PUBLICATION OR REPORT NUMBER
NISTIR 4929

2. PERFORMING ORGANIZATION REPORT NUMBER

3. PUBLICATION DATE
September 1992

4. TITLE AND SUBTITLE
Electronics and Electrical Engineering Laboratory Technical Publication Announcements Covering Laboratory Programs, October to December 1991, with 1992/1993 EEEL Events Calendar

5. AUTHOR(S)
J. A. Gonzalez, compiler

6. PERFORMING ORGANIZATION (IF JOINT OR OTHER THAN NIST, SEE INSTRUCTIONS)
U.S. DEPARTMENT OF COMMERCE
NATIONAL INSTITUTE OF STANDARDS AND TECHNOLOGY
GAITHERSBURG, MD 20899

7. CONTRACT/GRANT NUMBER

8. TYPE OF REPORT AND PERIOD COVERED
October-December 1991

9. SPONSORING ORGANIZATION NAME AND COMPLETE ADDRESS (STREET, CITY, STATE, ZIP)
U.S. Department of Commerce
National Institute of Standards and Technology
Electronics and Electrical Engineering Laboratory

10. SUPPLEMENTARY NOTES

11. ABSTRACT (A 200-WORD OR LESS FACTUAL SUMMARY OF MOST SIGNIFICANT INFORMATION. IF DOCUMENT INCLUDES A SIGNIFICANT BIBLIOGRAPHY OR LITERATURE SURVEY, MENTION IT HERE.)

This is the thirty-first issue of a quarterly publication providing information on the technical work of the National Institute of Standards and Technology, Electronics and Electrical Engineering Laboratory. This issue of the EEEL Technical Publication Announcements covers the fourth quarter of calendar year 1991. Abstracts are provided by technical area for papers published this quarter.

12. KEY WORDS (6 TO 12 ENTRIES; ALPHABETICAL ORDER; CAPITALIZE ONLY PROPER NAMES; AND SEPARATE KEY WORDS BY SEMICOLONS)

antennas; electrical engineering; electrical power; electromagnetic interference; electronics; instrumentation; laser; magnetics; microwave; optical fibers; semiconductors; superconductors

13. AVAILABILITY

X	UNLIMITED
	FOR OFFICIAL DISTRIBUTION. DO NOT RELEASE TO NATIONAL TECHNICAL INFORMATION SERVICE (NTIS).
	ORDER FROM SUPERINTENDENT OF DOCUMENTS, U.S. GOVERNMENT PRINTING OFFICE, WASHINGTON, DC 20402.
X	ORDER FROM NATIONAL TECHNICAL INFORMATION SERVICE (NTIS), SPRINGFIELD, VA 22161.

14. NUMBER OF PRINTED PAGES
34

15. PRICE
A03

ELECTRONIC FORM

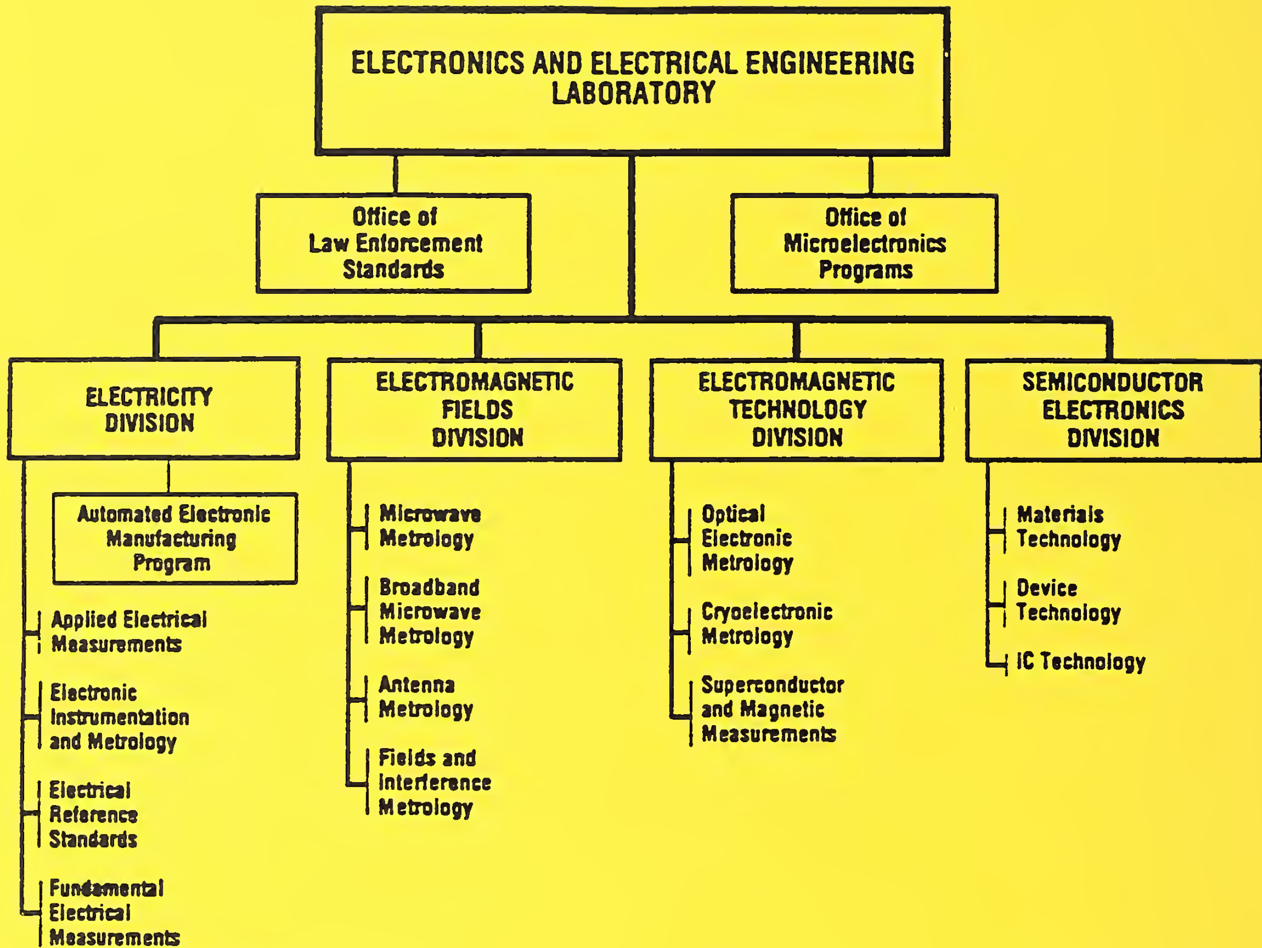

KEY CONTACTS

Laboratory Headquarters (810)	Director, Mr. Judson C. French (301) 975-2220
	Deputy Director, Dr. Robert E. Hebner (301) 975-2220
Office of Microelectronics Programs	Director, Mr. Robert I. Scace (301) 975-4400
Office of Law Enforcement Standards	Director, Mr. Lawrence K. Eliason (301) 975-2757
Electricity Division (811)	Chief, Dr. Oskars Petersons (301) 975-2400
Semiconductor Electronics Division (812)	Chief, Mr. Frank F. Oettinger (301) 975-2054
Electromagnetic Fields Division (813)	Chief, Mr. Allen C. Newell (303) 497-3131
Electromagnetic Technology Division (814)	Chief, Dr. Robert A. Kamper (303) 497-3535

INFORMATION:

For additional information on the Electronics and Electrical Engineering Laboratory, write or call:

Electronics and Electrical Engineering Laboratory
National Institute of Standards and Technology
Metrology Building, Room B-358
Gaithersburg, MD 20899
Telephone: (301) 975-2220